

Interstellar Medium (ISM)

Week 7

May 07 (Thursday), 2020

updated 05/06, 16:41

선광일 (Kwangil Seon)
KASI / UST

H II Regions 2 / WIM

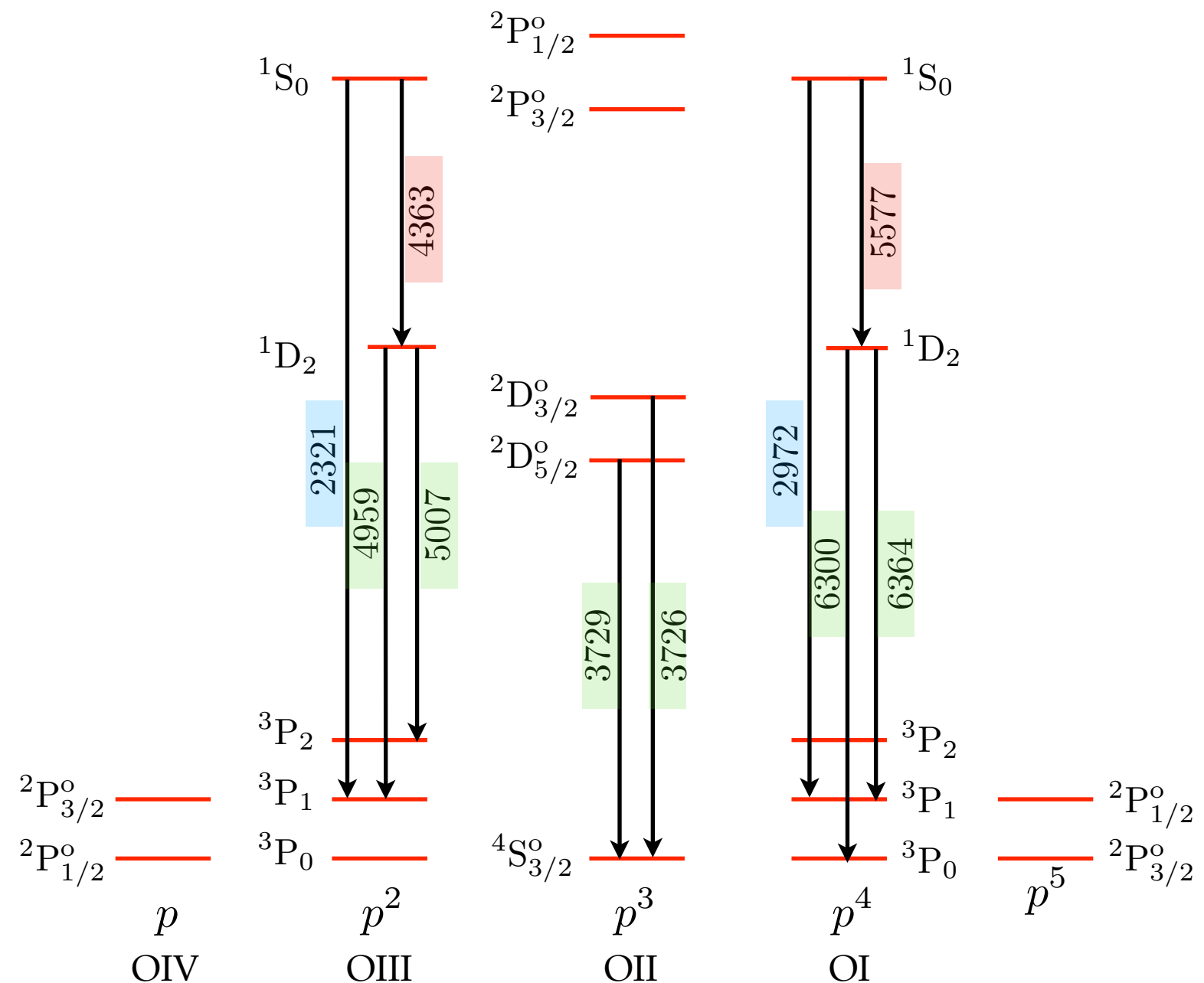
- Diagnostics & BPT diagram
 - Dynamics of H II regions
- Warm Ionized Medium, Diffuse Ionized Gas

Nebular, Auroral Lines

- Definitions:

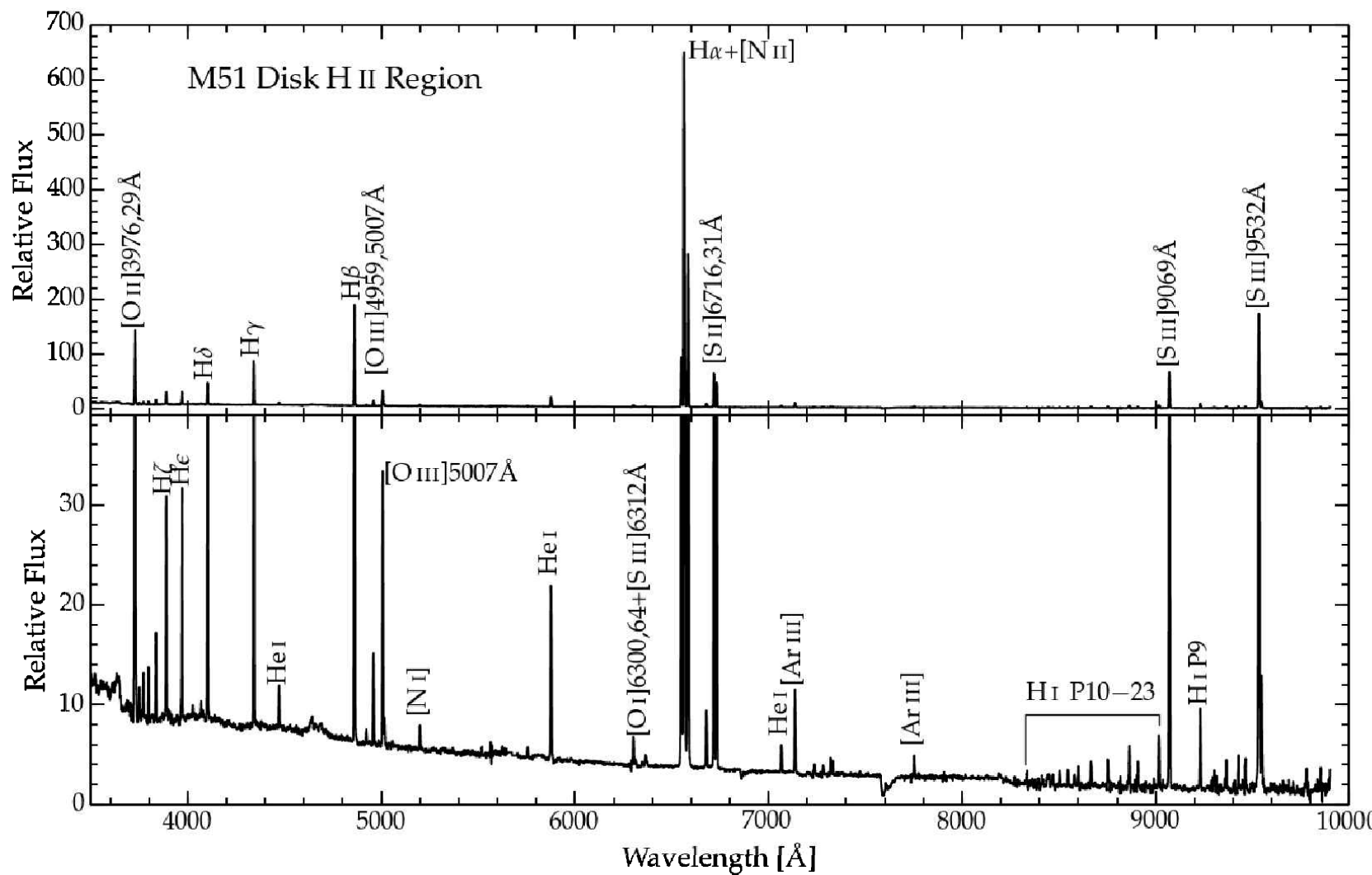
- **Auroral**: the transitions between ***two higher terms*** of configurations p^2 , p^3 , and p^4 are named auroral.
- **Nebular**: the transitions between ***the middle and the lowest terms*** give nebular lines.
- **Transauroral**: the transitions between ***the highest and the lowest terms*** give the transauroral lines.

The term structure for the ground configurations with p , p^2 , p^3 , p^4 , and p^5 outermost shells.
(not to scale)



Temperature, Density & Abundance Diagnostics

- In the figure, the continuum is a mixture of free-bound continuum (from radiative recombination), free-free emission (thermal bremsstrahlung), and two-photon emission.
- If we know enough about the temperature dependence of these continuum radiation, we can estimate the nebula temperature. However, the ***collisionally excited emission lines*** are much stronger than the continuum spectrum.



Spectrum of a disk HII region in the Whirlpool galaxy (M51).

(top) bright lines

(bottom) scaled to show faint lines.

Figure 4.6 [Ryden]

Temperature Determination

- The key to using emission lines to estimate temperature is finding two excited states of the same ion whose energy differs by $\sim kT$. For nebulae with $T \sim 10^4$ K, this implies energy differences of order of 1 eV or so.
- Atoms and ions with six electrons have $2p^2$ as their lowest configuration, and have 3 terms, as shown in the figure. Because the energy difference between the terms are very different. The relative strengths of the emission lines will be very sensitive to temperature.
- The measured intensity ratio can be used to determine the nebula temperature.

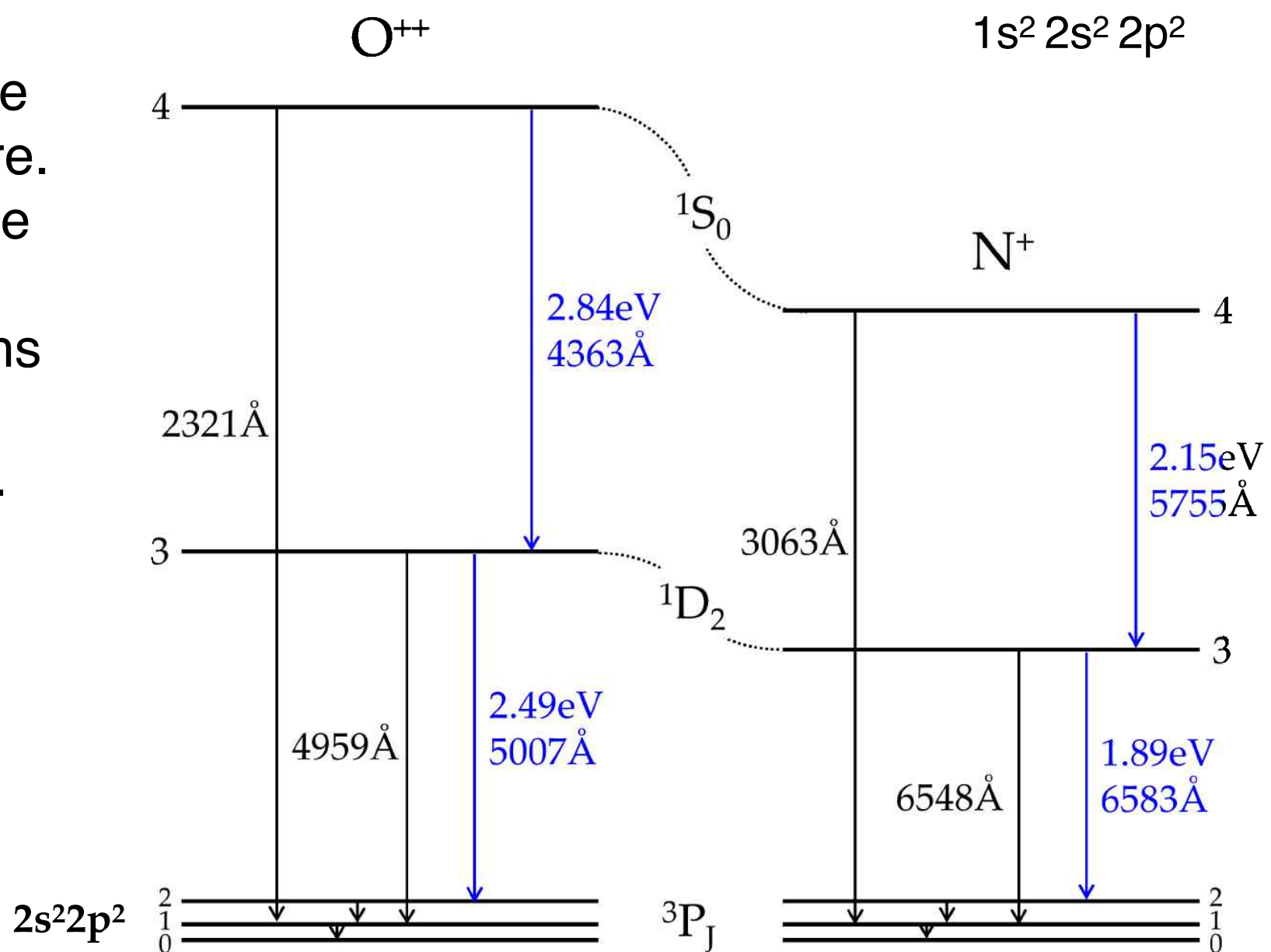


Figure 4.7 [Ryden]

$1s^2 2s^2 2p^2$

[O III]

[N II]

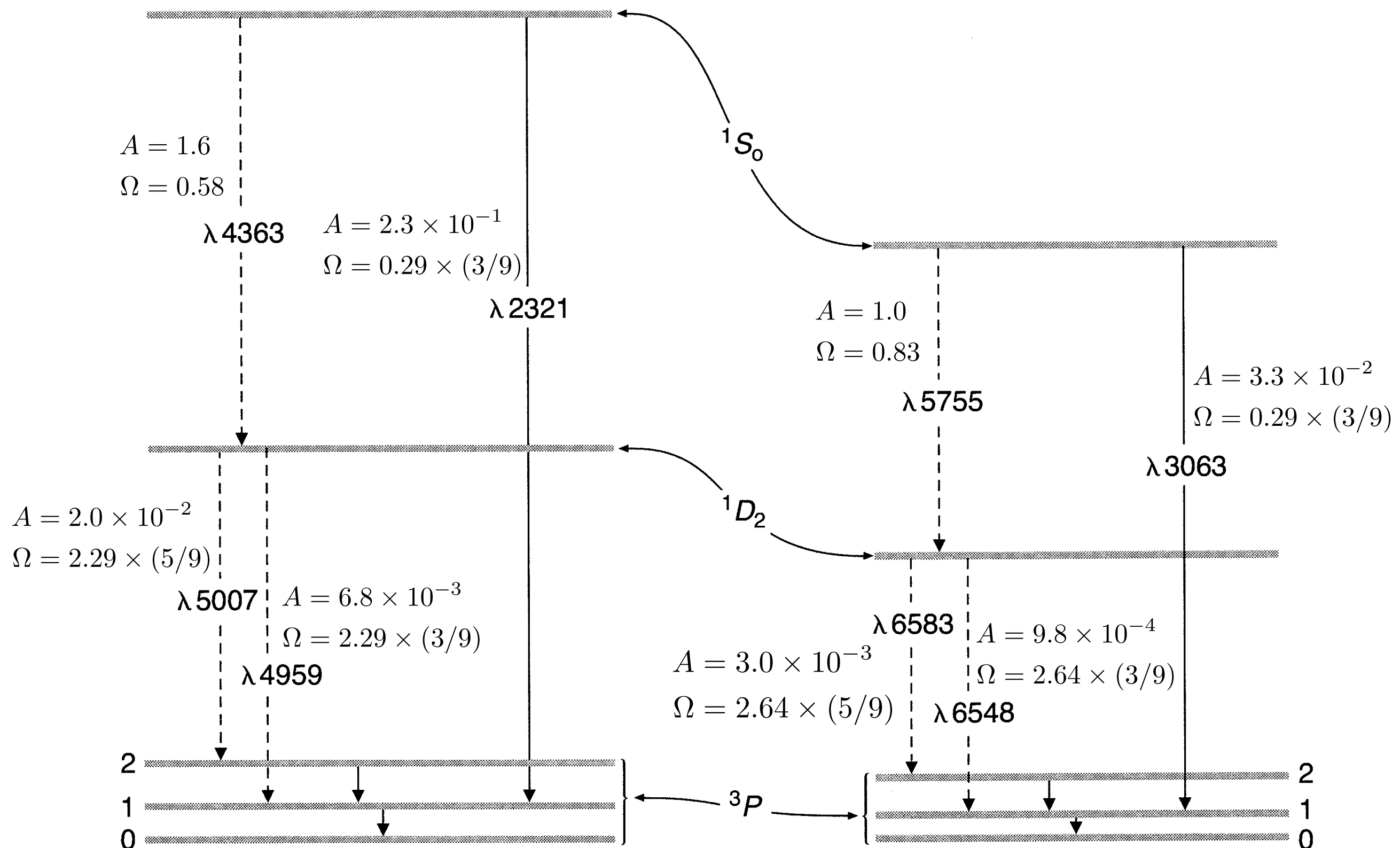


Figure 3.1 [Osterbrock]
Astrophysics of Gaseous Nebulae
and Active Galactic Nuclei

See Table 3.12 for A and
Table 3.6 for Collision Strength

Ion	3P , 1D	3P , 1S	1D , 1S
N^+	2.64	0.29	0.83
O^{+2}	2.29	0.29	0.58

Table 3.6
Collision Strength

-
- Candidate 2p² ions are C I, N II, O III, F IV, Ne V, and so on.
 - C I is easily photo ionized, and will have very low abundance in an H II region.
 - F IV, Ne VI,... have an ionization potential exceeding 54.4 eV, and we do not expect such high ionization states to be abundant in H II regions.
 - This leaves N II and O III as the only 2p² ions that will be available in H II regions.
 - The lowest excited states of singly ionized nitrogen (N II) and doubly ionized oxygen (O III) are useful tools for estimating the temperatures of H II regions and planetary nebulae.
 - N II and O III have six bound electrons, and thus their fine structure energy levels in their lowest configuration are very similar in structure.

p ² Ions	[N II]	[O III]	[Ne V]	[S III]
$^1S_0 \rightarrow ^1D_2$	5755	4363	2974	6312
$^1D_2 \rightarrow ^3P_2$	6583	5007	3426	9532
$^1D_2 \rightarrow ^3P_1$	6548	4959	3346	9069

p ⁴ Ions	[O I]	[Ne III]	[Ar III]
$^1S_0 \rightarrow ^1D_2$	5577	3343	5192
$^1D_2 \rightarrow ^3P_2$	6300	3869	7136
$^1D_2 \rightarrow ^3P_1$	6363	3968	7751

Temperature-sensitive nebular lines (Å).

- Let's suppose that we are in the low-density limit, so that the free electron density is less than the critical density for collisional de-excitation of each line. In this case, every collisional excitation will be followed by radiative decays returning the ion to the ground state, with branching ratios that are determined by the Einstein coefficients.

- $4 \rightarrow 3$ transition:

- ▶ The emissivity of the $4 \rightarrow 3$ transition, integrated over the entire line width is:

$$4\pi j(4 \rightarrow 3) = n_4 A_{43} h\nu_{43}$$

- ▶ The rate of collisional excitation from “0” to level “4” is balanced by radiative de-excitation from “4” to “3” and “1”:

$$n_e n_0 k_{04} = n_4 (A_{43} + A_{41})$$

- ▶ Therefore,

$$4\pi j(4 \rightarrow 3) = n_e n_0 k_{04} \frac{A_{43}}{A_{43} + A_{41}} h\nu_{43}$$

-
- $3 \rightarrow 2$ transition:
 - ▶ The level “3” can be populated in two ways: (1) by collisional excitation directly from the ground state, and (2) by a collisional excitation from the ground to “4”, followed by radiative de-excitation to “3”.

$$4\pi j(3 \rightarrow 2) = n_e n_0 \left(k_{03} + k_{04} \frac{A_{43}}{A_{43} + A_{41}} \right) \frac{A_{32}}{A_{32} + A_{31}} h\nu_{32}$$

- The relative strength between $4 \rightarrow 3$ and $3 \rightarrow 2$ emission line:

$$\frac{j(4 \rightarrow 3)}{j(3 \rightarrow 2)} = \frac{A_{43}}{A_{32}} \frac{\nu_{43}}{\nu_{32}} \frac{(A_{32} + A_{31})k_{04}}{(A_{43} + A_{41})k_{03} + A_{43}k_{04}}$$

- We notice that the temperature dependence in the above equation enters solely through the collisional rate coefficients k_{04} and k_{03} . Using the relation between the collisional excitation and de-excitation rate coefficients,

$$\begin{aligned} k_{0u} &= k_{u0} \frac{g_u}{g_0} e^{-h\nu_{u0}/kT} \\ &= \frac{\beta}{g_0} \frac{\langle \Omega_{u0} \rangle}{T^{1/2}} e^{-h\nu_{u0}/kT} \end{aligned}$$

- We obtain

$$\frac{j(4 \rightarrow 3)}{j(3 \rightarrow 2)} = \frac{A_{43}}{A_{32}} \frac{\nu_{43}}{\nu_{32}} \frac{(A_{32} + A_{31}) \langle \Omega_{40} \rangle e^{-h\nu_{43}/kT}}{(A_{43} + A_{41}) \langle \Omega_{30} \rangle + A_{43} \langle \Omega_{40} \rangle e^{-h\nu_{43}/kT}}$$

where $h\nu_{43} = h\nu_{40} - h\nu_{30}$

- Notice that all the temperature dependence, aside from the weak dependence of collision strengths on temperature, is contained in the exponential factor. Thus, the line ratio is sensitive to the temperature $kT \sim h\nu_{43}$ (2.15 eV for N II, 2.84 eV for O III).
- At the high and low temperatures, the ratio can be expressed as

$$\begin{aligned} \frac{j(4 \rightarrow 3)}{j(3 \rightarrow 2)} &\approx \frac{A_{43}}{A_{32}} \frac{\nu_{43}}{\nu_{32}} \frac{(A_{32} + A_{31}) \langle \Omega_{40} \rangle}{(A_{43} + A_{41}) \langle \Omega_{30} \rangle + A_{43} \langle \Omega_{40} \rangle} \quad \text{for } kT \gg h\nu_{43} \\ &\approx \frac{A_{43}}{A_{32}} \frac{\nu_{43}}{\nu_{32}} \frac{(A_{32} + A_{31}) \langle \Omega_{40} \rangle}{(A_{43} + A_{41}) \langle \Omega_{30} \rangle} e^{-h\nu_{43}/kT} \quad \text{for } kT \ll h\nu_{43} \end{aligned}$$

At high temperatures, the line ratio becomes more or less independent of temperature.

$$\frac{j(4 \rightarrow 3)}{j(3 \rightarrow 2)} = \frac{A_{43}}{A_{32}} \frac{\nu_{43}}{\nu_{32}} \frac{(A_{32} + A_{31}) \langle \Omega_{40} \rangle e^{-h\nu_{43}/kT}}{(A_{43} + A_{41}) \langle \Omega_{30} \rangle + A_{43} \langle \Omega_{40} \rangle e^{-h\nu_{43}/kT}}$$

Dependence of collision strength on temperature is very weak.
So, we will adopt a typical value.

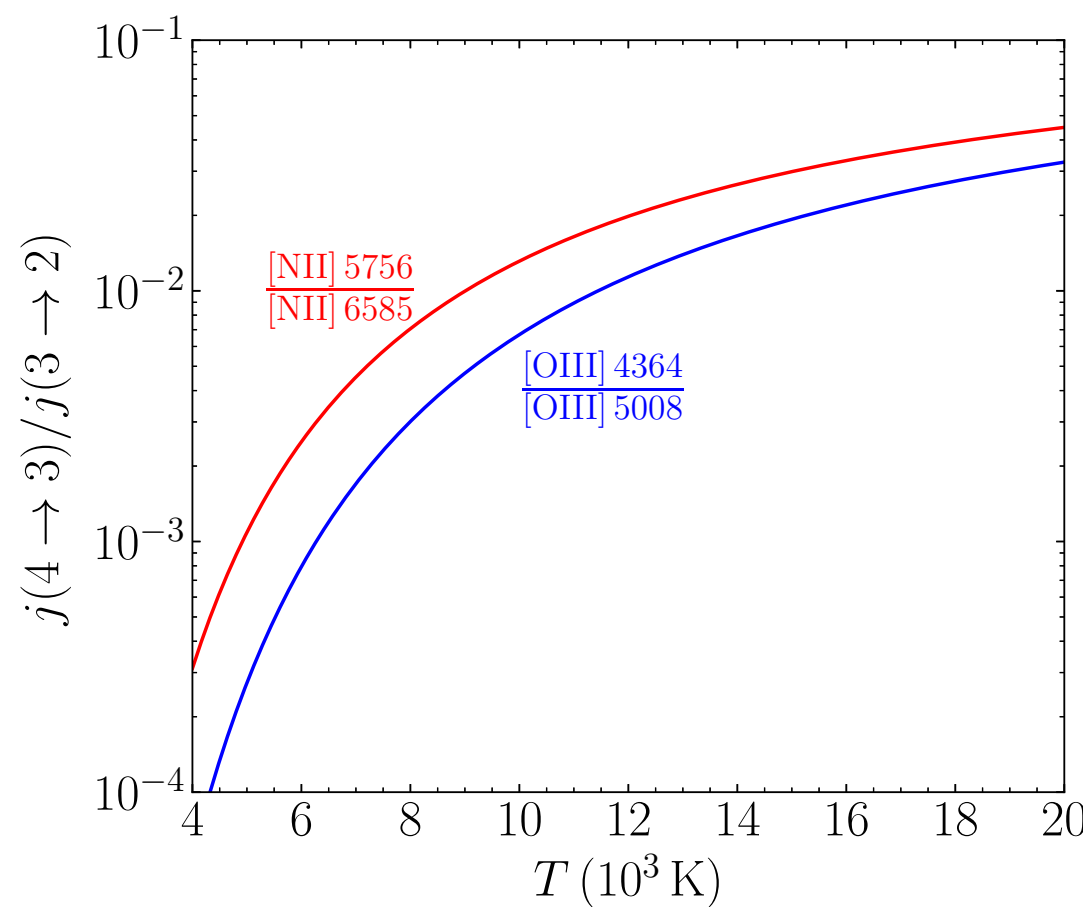
$$T_4 \equiv T/10^4 \text{ K}$$

[O III]	$\langle \Omega_{30} \rangle = 2.29 \times (1/9)$	$A_{32} = 2.0 \times 10^{-2} \text{ [s}^{-1}\text{]}$
	$\langle \Omega_{40} \rangle = 0.29 \times (1/9)$	$A_{31} = 6.8 \times 10^{-3} \text{ [s}^{-1}\text{]}$
	$E_{40}/k = 61207 \text{ [K]}$	$A_{43} = 1.6 \text{ [s}^{-1}\text{]}$
	$E_{30}/k = 29169 \text{ [K]}$	$A_{41} = 2.3 \times 10^{-1} \text{ [s}^{-1}\text{]}$
	$E_{20}/k = 441 \text{ [K]}$	
	$E_{10}/k = 163 \text{ [K]}$	

$$\frac{j(4364)}{j(5008)} = 0.1655 \frac{e^{-3.2038/T_4}}{1 + 0.1107e^{-3.2038/T_4}}$$

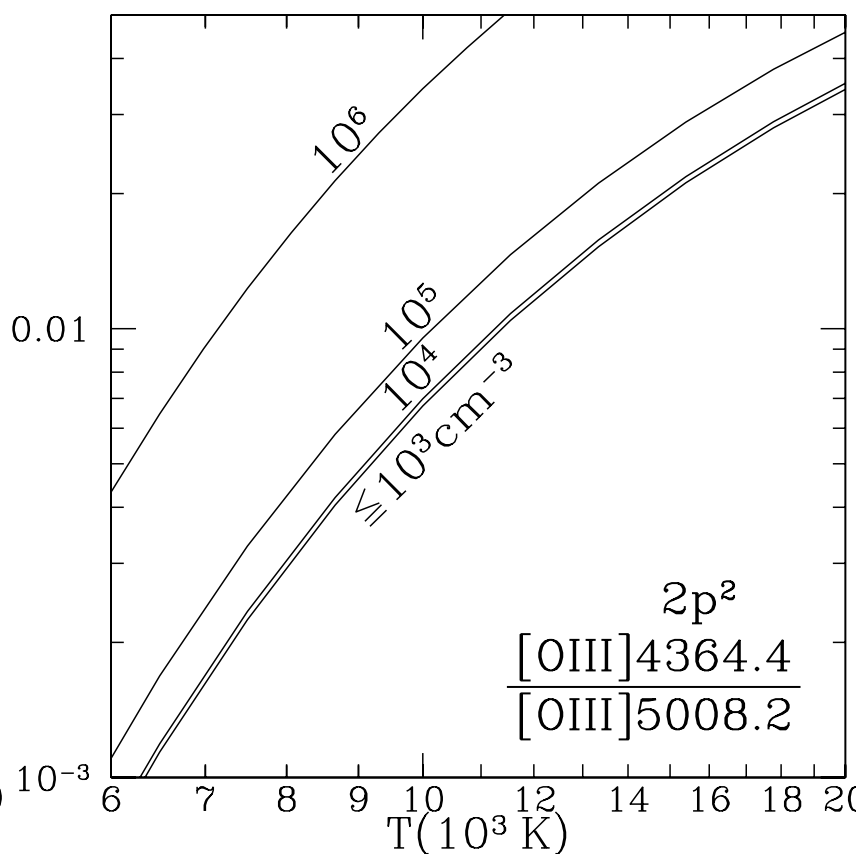
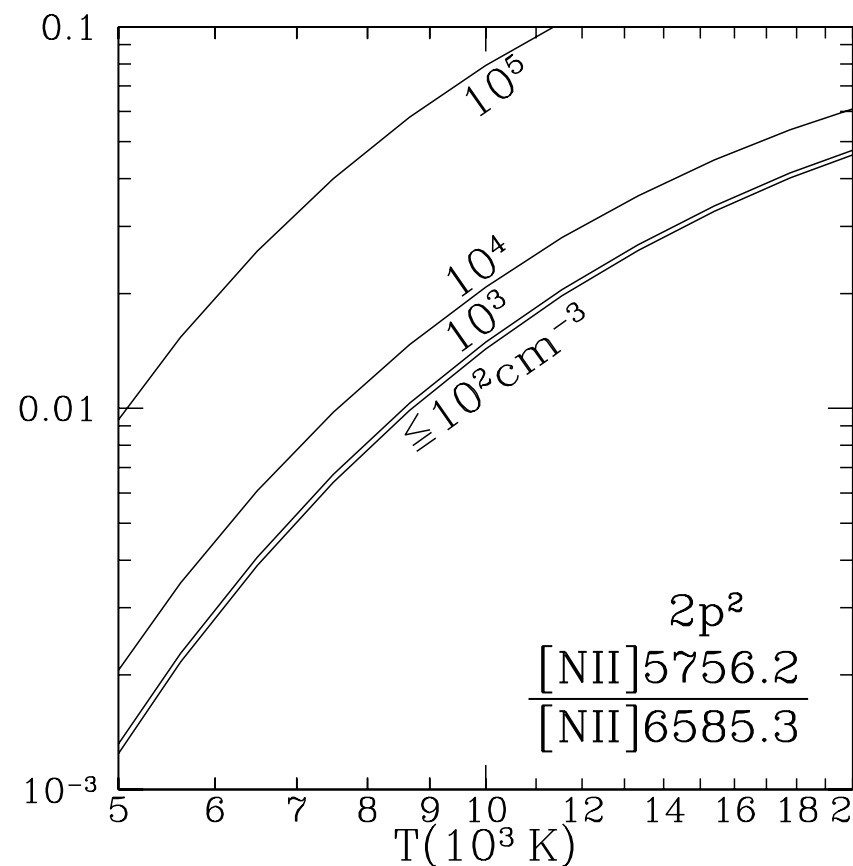
[N II]	$\langle \Omega_{30} \rangle = 2.64 \times (1/9)$	$A_{32} = 3.0 \times 10^{-3} \text{ [s}^{-1}\text{]}$
	$\langle \Omega_{40} \rangle = 0.29 \times (1/9)$	$A_{31} = 9.8 \times 10^{-4} \text{ [s}^{-1}\text{]}$
	$E_{40}/k = 47033 \text{ [K]}$	$A_{43} = 1.0 \text{ [s}^{-1}\text{]}$
	$E_{30}/k = 22037 \text{ [K]}$	$A_{41} = 3.3 \times 10^{-2} \text{ [s}^{-1}\text{]}$
	$E_{20}/k = 188 \text{ [K]}$	
	$E_{10}/k = 70 \text{ [K]}$	

$$\frac{j(5756)}{j(6585)} = 0.1614 \frac{e^{-2.4996/T_4}}{1 + 0.1063e^{-2.4996/T_4}}$$



Line ratios as a function of temperature, which is obtained using the equations in the previous slide.

[O III] 4364Å is called the auroral line. Unfortunately, the auroral line at 4364Å can only be observed when the temperature is sufficiently high.



Line ratios for temperature diagnostics.

Curves indicate electron density. For each ion, the low density limit is shown, as well as results for higher densities.

Figure 18.2 [Draine]

-
- Sometimes, it would be better to combine $3 \rightarrow 2$ and $3 \rightarrow 1$ transitions:

- $3 \rightarrow 1$ transition:

$$4\pi j(3 \rightarrow 2) = n_e n_0 \left(k_{03} + k_{04} \frac{A_{43}}{A_{43} + A_{41}} \right) \frac{A_{32}}{A_{32} + A_{31}} h\nu_{32}$$

$$4\pi j(3 \rightarrow 1) = n_e n_0 \left(k_{03} + k_{04} \frac{A_{43}}{A_{43} + A_{41}} \right) \frac{A_{31}}{A_{32} + A_{31}} h\nu_{31}$$

$$4\pi [j(3 \rightarrow 1) + j(3 \rightarrow 2)] = n_e n_0 \left(k_{03} + k_{04} \frac{A_{43}}{A_{43} + A_{41}} \right) h\bar{\nu} \quad \text{where } \bar{\nu} \equiv \frac{A_{32}\nu_{32} + A_{31}\nu_{31}}{A_{32} + A_{31}}$$

- Recall that

$$4\pi j(4 \rightarrow 3) = n_e n_0 k_{04} \frac{A_{43}}{A_{43} + A_{41}} h\nu_{43}$$

Combining these equations, we obtain

$$\frac{j(3 \rightarrow 1) + j(3 \rightarrow 2)}{j(4 \rightarrow 3)} = \frac{\bar{\nu}}{\nu_{43}} \frac{A_{43} + A_{41}}{A_{43}} \frac{k_{03}}{k_{04}} \left(1 + \frac{k_{04}}{k_{03}} \frac{A_{43}}{A_{43} + A_{41}} \right)$$

$$k_{0u} = \frac{\beta}{T^{1/2}} \frac{\langle \Omega_{u0} \rangle}{g_0} e^{-E_{u0}/kT_{\text{gas}}}$$

↓

$$\frac{k_{03}}{k_{04}} = \frac{\langle \Omega_{30} \rangle}{\langle \Omega_{40} \rangle} \frac{e^{-h\nu_{30}/kT}}{e^{-h\nu_{40}/kT}} = \frac{\langle \Omega_{30} \rangle}{\langle \Omega_{40} \rangle} e^{h\nu_{43}/kT} \quad (\text{where } \nu_{43} = \nu_{40} - \nu_{30})$$

$$\begin{aligned} \frac{j(3 \rightarrow 1) + j(3 \rightarrow 2)}{j(4 \rightarrow 3)} &= \frac{\bar{\nu}}{\nu_{43}} \frac{A_{43} + A_{41}}{A_{43}} \frac{\langle \Omega_{30} \rangle}{\langle \Omega_{40} \rangle} e^{h\nu_{43}/kT} \left(1 + \frac{\langle \Omega_{40} \rangle}{\langle \Omega_{30} \rangle} \frac{A_{43}}{A_{43} + A_{41}} e^{-h\nu_{43}/kT} \right) \\ &\simeq \frac{\bar{\nu}}{\nu_{43}} \frac{A_{43} + A_{41}}{A_{43}} \frac{\langle \Omega_{30} \rangle}{\langle \Omega_{40} \rangle} e^{h\nu_{43}/kT} \end{aligned}$$

Note $\langle \Omega_{40} \rangle < \langle \Omega_{30} \rangle$ and $e^{-h\nu_{43}/kT} \ll 1$.

Thus, the term inside the parenthesis is negligible.

$$\frac{j(3 \rightarrow 1) + j(3 \rightarrow 2)}{j(4 \rightarrow 3)} \simeq \frac{\bar{\nu}}{\nu_{43}} \frac{A_{43} + A_{41}}{A_{43}} \frac{\langle \Omega_{30} \rangle}{\langle \Omega_{40} \rangle} e^{h\nu_{43}/kT}$$

Use the following data:

[O III]	$\langle \Omega_{30} \rangle = 2.29 \times (1/9)$	$A_{32} = 2.0 \times 10^{-2} \text{ [s}^{-1}\text{]}$
	$\langle \Omega_{40} \rangle = 0.29 \times (1/9)$	$A_{31} = 6.8 \times 10^{-3} \text{ [s}^{-1}\text{]}$
	$E_{40}/k = 61207 \text{ [K]}$	$A_{43} = 1.6 \text{ [s}^{-1}\text{]}$
	$E_{30}/k = 29169 \text{ [K]}$	$A_{41} = 2.3 \times 10^{-1} \text{ [s}^{-1}\text{]}$
	$E_{20}/k = 441 \text{ [K]}$	
	$E_{10}/k = 163 \text{ [K]}$	

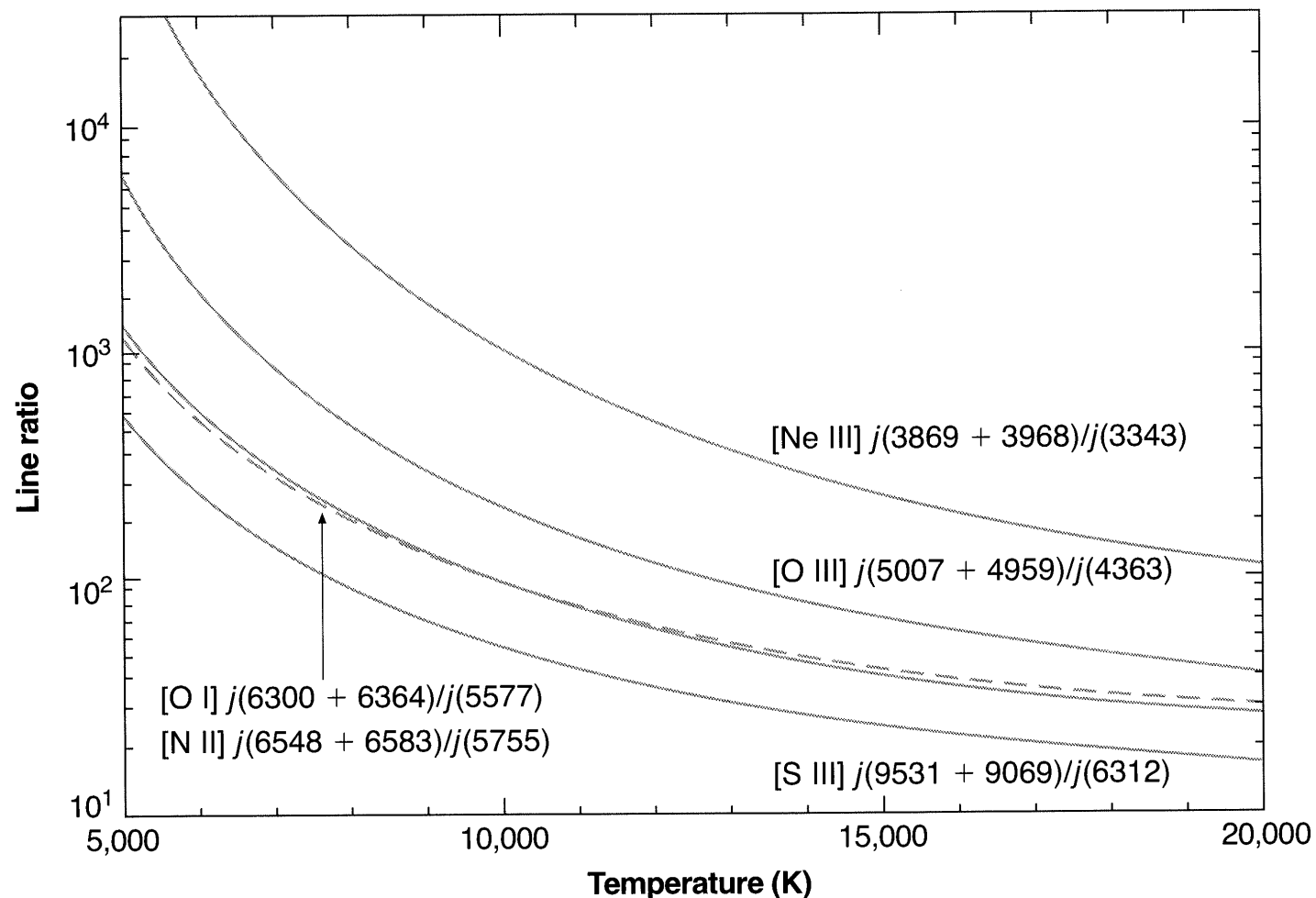
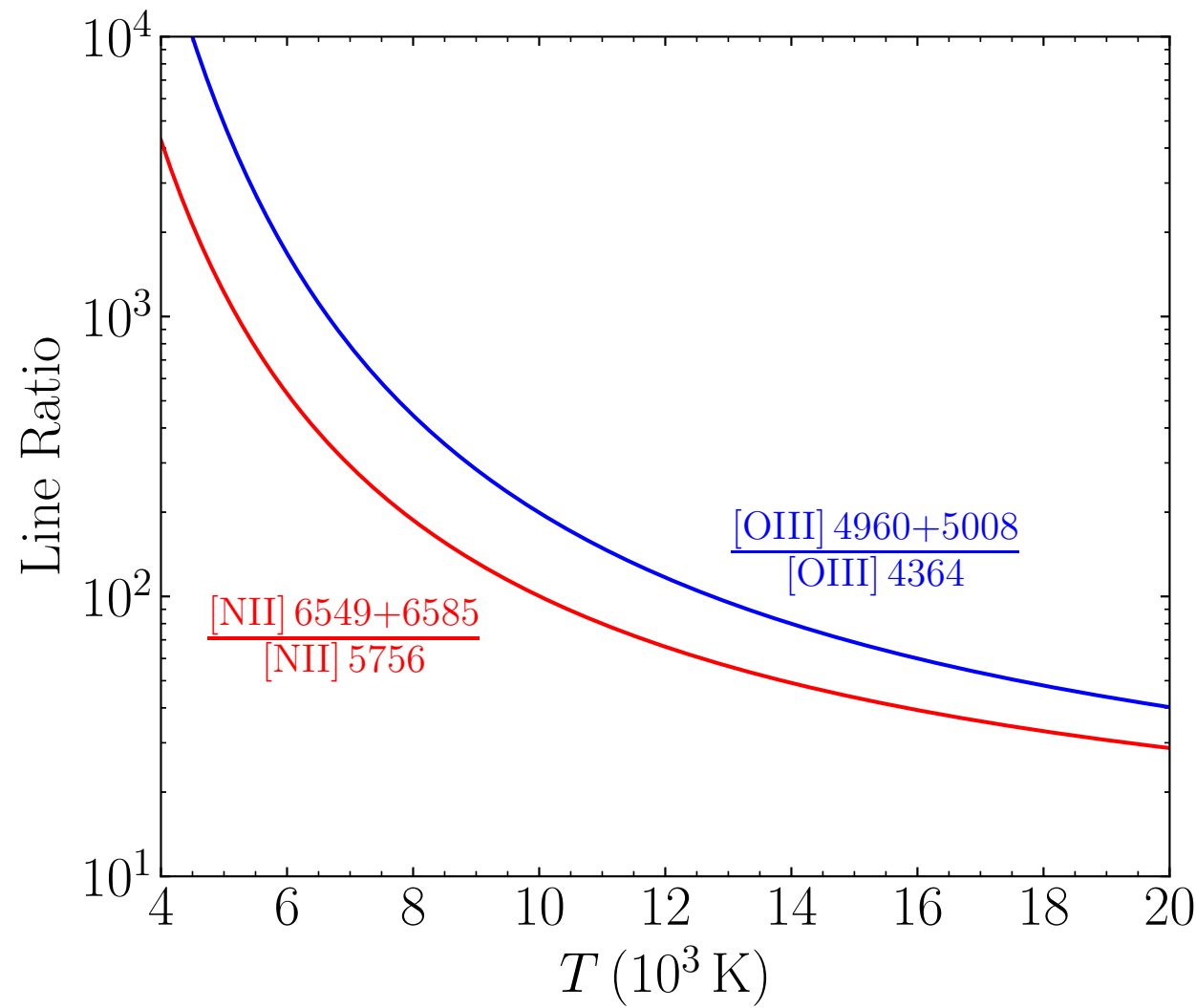
[N II]	$\langle \Omega_{30} \rangle = 2.64 \times (1/9)$	$A_{32} = 3.0 \times 10^{-3} \text{ [s}^{-1}\text{]}$
	$\langle \Omega_{40} \rangle = 0.29 \times (1/9)$	$A_{31} = 9.8 \times 10^{-4} \text{ [s}^{-1}\text{]}$
	$E_{40}/k = 47033 \text{ [K]}$	$A_{43} = 1.0 \text{ [s}^{-1}\text{]}$
	$E_{30}/k = 22037 \text{ [K]}$	$A_{41} = 3.3 \times 10^{-2} \text{ [s}^{-1}\text{]}$
	$E_{20}/k = 188 \text{ [K]}$	
	$E_{10}/k = 70 \text{ [K]}$	

We obtain the line ratio as a function of temperature.

$$\frac{[\text{O III}] 4960 + 5008}{[\text{O III}] 4364} = 8.12 e^{3.20/T_4}$$

$$\frac{[\text{N II}] 6549 + 6585}{[\text{N II}] 5756} = 8.23 e^{2.50/T_4}$$

Figure 5.1 [Osterbrock]



$$[\text{O III}] \frac{j_{\lambda 4959} + j_{\lambda 5007}}{j_{\lambda 4363}} = \frac{7.90 \exp(3.29 \times 10^4/T)}{1 + 4.5 \times 10^{-4} n_e / T^{1/2}}$$

$$[\text{N II}] \frac{j_{\lambda 6548} + j_{\lambda 6583}}{j_{\lambda 5755}} = \frac{8.23 \exp(2.50 \times 10^4/T)}{1 + 4.4 \times 10^{-3} n_e / T^{1/2}}$$

$$[\text{Ne III}] \frac{j_{\lambda 3869} + j_{\lambda 3968}}{j_{\lambda 3343}} = \frac{13.7 \exp(4.30 \times 10^4/T)}{1 + 3.8 \times 10^{-5} n_e / T^{1/2}}$$

$$[\text{S III}] \frac{j_{\lambda 9532} + j_{\lambda 9069}}{j_{\lambda 6312}} = \frac{5.44 \exp(2.28 \times 10^4/T)}{1 + 3.5 \times 10^{-4} n_e / T^{1/2}}$$

See Equations (5.4)-(5.7) for a correction factor due to the density effect.

Density Determination

- Emission lines can also be used to estimate the free electron density of an ionized nebula. For this purpose, we need an ion which has two excited levels that are similar in energy, but which have different critical densities. One of such systems is singly-ionized oxygen.
- Ions with 7 or 15 electrons have $2s^22p^3$ and $3s^23p^3$ configurations, with energy level structures that make them suitable for use as density diagnostics.

Density-sensitive nebular lines (Å).

p ³ Ions	[O II]	[S II]	[Ne IV]	[Ar IV]
$^2D_{3/2} \rightarrow ^4S_{3/2}$	3726	6731	2423	4740
$^2D_{5/2} \rightarrow ^4S_{3/2}$	3729	6716	2426	4711

Table 3.7 [Osterbrock]

Ion	$^4S^o$, $^2D^o$
O ⁺	1.34
Ne ⁺³	1.40
S ⁺	6.90
Ar ⁺³	1.90

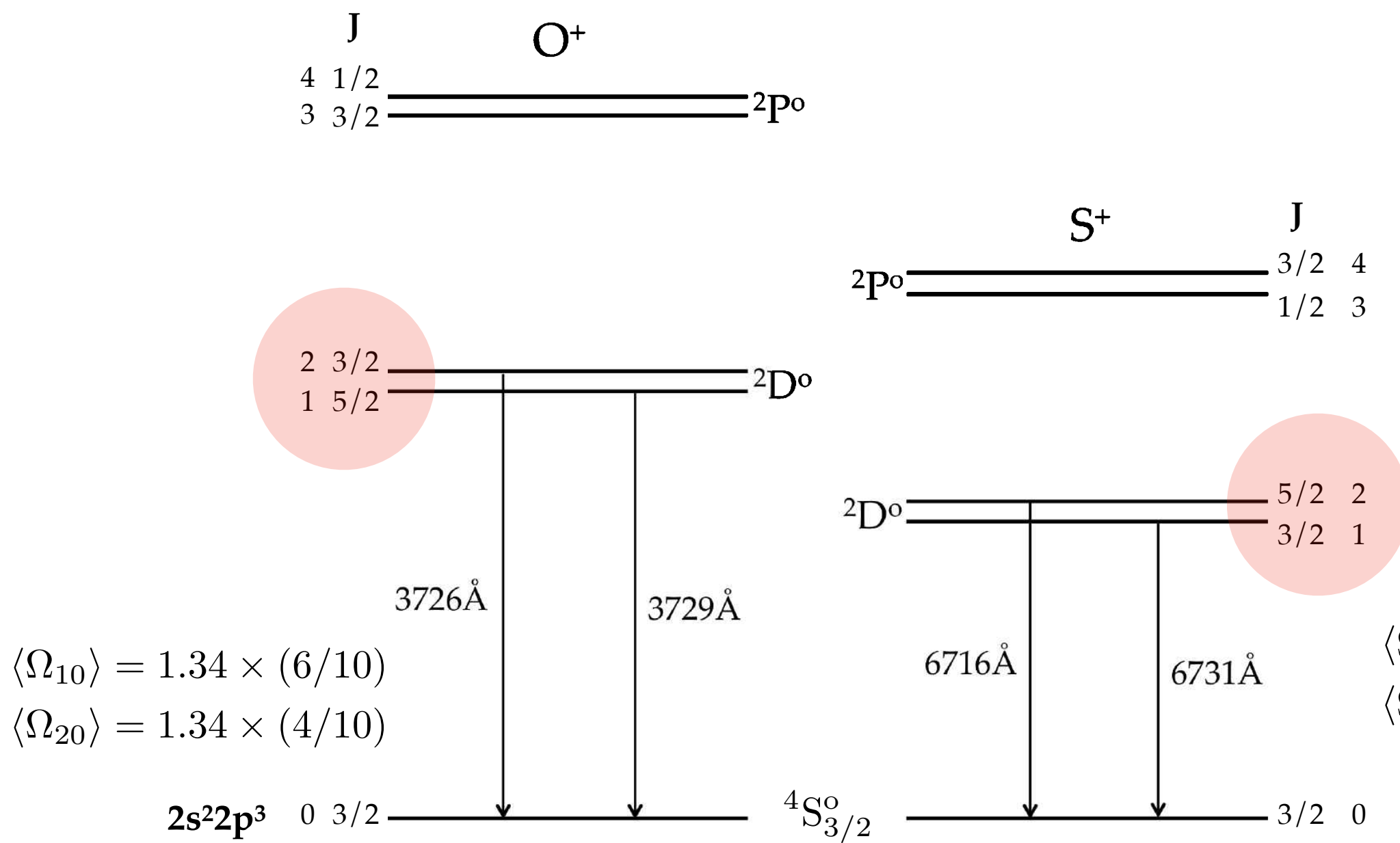


Figure 4.8 [Ryden]

Notice that energy ordering of the fine-structure levels are different between O⁺ and S⁺. The 2p configuration for the two ions are half-filled, and thus **Hund's rule for the energy ordering is not applicable**.

There are three typos in J values for S⁺ and in the notation for the lowest level in Figure 4.8 of [Ryden].

-
- Here, we ignore the transition between 2 and 1.
 - $1 \rightarrow 0$ transition:
 - The emissivity of the $1 \rightarrow 0$ transition, integrated over the entire line width, is

$$4\pi j(1 \rightarrow 0) = n_1 A_{10} h\nu_{10}$$

- In equilibrium, the rate of collisional excitation from the ground state will be balanced by radiative and collisional de-excitation:

$$n_e n_0 k_{01} = n_1 (A_{10} + n_e k_{10})$$

$$\begin{aligned} k_{0u} &= k_{u0} \frac{g_u}{g_0} e^{-h\nu_{u0}/kT} \\ &= \frac{\beta}{g_0} \frac{\langle \Omega_{u0} \rangle}{T^{1/2}} e^{-h\nu_{u0}/kT} \end{aligned}$$

- Then,

$$\begin{aligned} 4\pi j(1 \rightarrow 0) &= n_e n_0 \frac{k_{01}}{A_{10} + n_e k_{10}} A_{10} h\nu_{10} \\ &= n_e n_0 \frac{k_{01}}{1 + n_e/n_{\text{crit},1}} h\nu_{10} \end{aligned}$$

where $n_{\text{crit},1} = A_{10}/k_{10}$

- $2 \rightarrow 0$ transition:
 - Similarly, we obtain

$$4\pi j(2 \rightarrow 0) = n_e n_0 \frac{k_{02}}{1 + n_e/n_{\text{crit},2}} h\nu_{20}$$

where $n_{\text{crit},2} = A_{20}/k_{20}$

- The ratio of the strength of the two lines in the doublet is

$$\begin{aligned}\frac{j(2 \rightarrow 0)}{j(1 \rightarrow 0)} &= \frac{\nu_{20}}{\nu_{10}} \frac{k_{02}}{k_{01}} \frac{1 + n_e/n_{\text{crit},1}}{1 + n_e/n_{\text{crit},2}} \\ &= \frac{\nu_{20}}{\nu_{10}} \frac{\langle \Omega_{20} \rangle}{\langle \Omega_{10} \rangle} e^{-h\nu_{21}/kT} \frac{1 + n_e/n_{\text{crit},1}}{1 + n_e/n_{\text{crit},2}}\end{aligned}$$

$$k_{0u} = \left(\frac{\beta}{T^{1/2}} \frac{1}{g_0} \right) \langle \Omega_{u0} \rangle e^{-h\nu_{u0}/kT}$$

$$h\nu_{21} \equiv h\nu_{20} - h\nu_{10} \ll kT$$

$$h\nu_{21} \approx 2 \text{ meV} \quad \text{for O II ions}$$

- Thus, we can write the line ratio as

$$\frac{j(2 \rightarrow 0)}{j(1 \rightarrow 0)} \simeq \frac{\langle \Omega_{20} \rangle}{\langle \Omega_{10} \rangle} \frac{1 + n_e/n_{\text{crit},1}}{1 + n_e/n_{\text{crit},2}}$$

$h\nu_{20} \simeq h\nu_{10}$ since level 1 and 2 are so close in energy.

- In the low-density limit ($n_e \ll n_{\text{crit},1}, n_{\text{crit},2}$),

$$\frac{j(2 \rightarrow 0)}{j(1 \rightarrow 0)} \simeq \frac{\langle \Omega_{20} \rangle}{\langle \Omega_{10} \rangle} = \frac{g_2}{g_1}$$

$$\Omega_{(\text{SLJ}, \text{ S'L'J'})} = \frac{(2J'+1)}{(2S'+1)(2L'+1)} \Omega_{(\text{SL}, \text{ S'L'})}$$

Recall the sum rule for the collision strength for the fine-structure transitions.
 [However, it is not clear that the sum rule is valid even beyond the LS-coupling scheme. Recent numerical calculations show that the proportionality is only approximately.]

- In high-density limit ($n_e \gg n_{\text{crit},2}, n_{\text{crit},1}$),

$$\frac{j(2 \rightarrow 0)}{j(1 \rightarrow 0)} \simeq \frac{\langle \Omega_{20} \rangle}{\langle \Omega_{10} \rangle} \frac{n_{\text{crit},2}}{n_{\text{crit},1}} = \frac{\langle \Omega_{20} \rangle}{\langle \Omega_{10} \rangle} \frac{A_{20}/k_{20}}{A_{10}/k_{10}} = \frac{g_2}{g_1} \frac{A_{20}}{A_{10}}$$

$$k_{u0} = \frac{\beta}{T^{1/2}} \frac{\langle \Omega_{u0} \rangle}{g_u}$$

► For O II ion,

$$n_e \ll n_{\text{crit}} \rightarrow \frac{j(1 \rightarrow 0)}{j(2 \rightarrow 0)} \simeq \frac{g_1}{g_2}$$

$$n_e \gg n_{\text{crit}} \rightarrow \frac{j(1 \rightarrow 0)}{j(2 \rightarrow 0)} \simeq \frac{g_1}{g_2} \frac{A_{10}}{A_{20}}$$

$$\frac{j([\text{O II}] 3728.8)}{j([\text{O II}] 3726.1)} = 1.5$$

$$\frac{j([\text{O II}] 3728.8)}{j([\text{O II}] 3726.1)} = 0.3$$

$$g_1 = 6, \quad A_{10} = 3.59 \times 10^{-5} \text{ s}^{-1}$$

$$g_2 = 4, \quad A_{20} = 1.79 \times 10^{-4} \text{ s}^{-1}$$

$$\frac{j(3729)}{j(3726)} = 1.5 \frac{1 + (n_e / 1.55 \times 10^4 \text{ cm}^{-3}) T_4^{-1/2}}{1 + (n_e / 3.11 \times 10^3 \text{ cm}^{-3}) T_4^{-1/2}}$$

$$\langle \Omega_{10} \rangle = 1.34 \times (6/10)$$

$$\langle \Omega_{20} \rangle = 1.34 \times (4/10)$$

► For S II ion,

$$n_e \ll n_{\text{crit}} \rightarrow \frac{j(2 \rightarrow 0)}{j(1 \rightarrow 0)} \simeq \frac{g_2}{g_1}$$

$$n_e \gg n_{\text{crit}} \rightarrow \frac{j(2 \rightarrow 0)}{j(1 \rightarrow 0)} \simeq \frac{g_2}{g_1} \frac{A_{20}}{A_{10}}$$

$$\frac{j([\text{S II}] 6716)}{j([\text{S II}] 6731)} = 1.5$$

$$\frac{j([\text{S II}] 6716)}{j([\text{S II}] 6731)} = 0.44$$

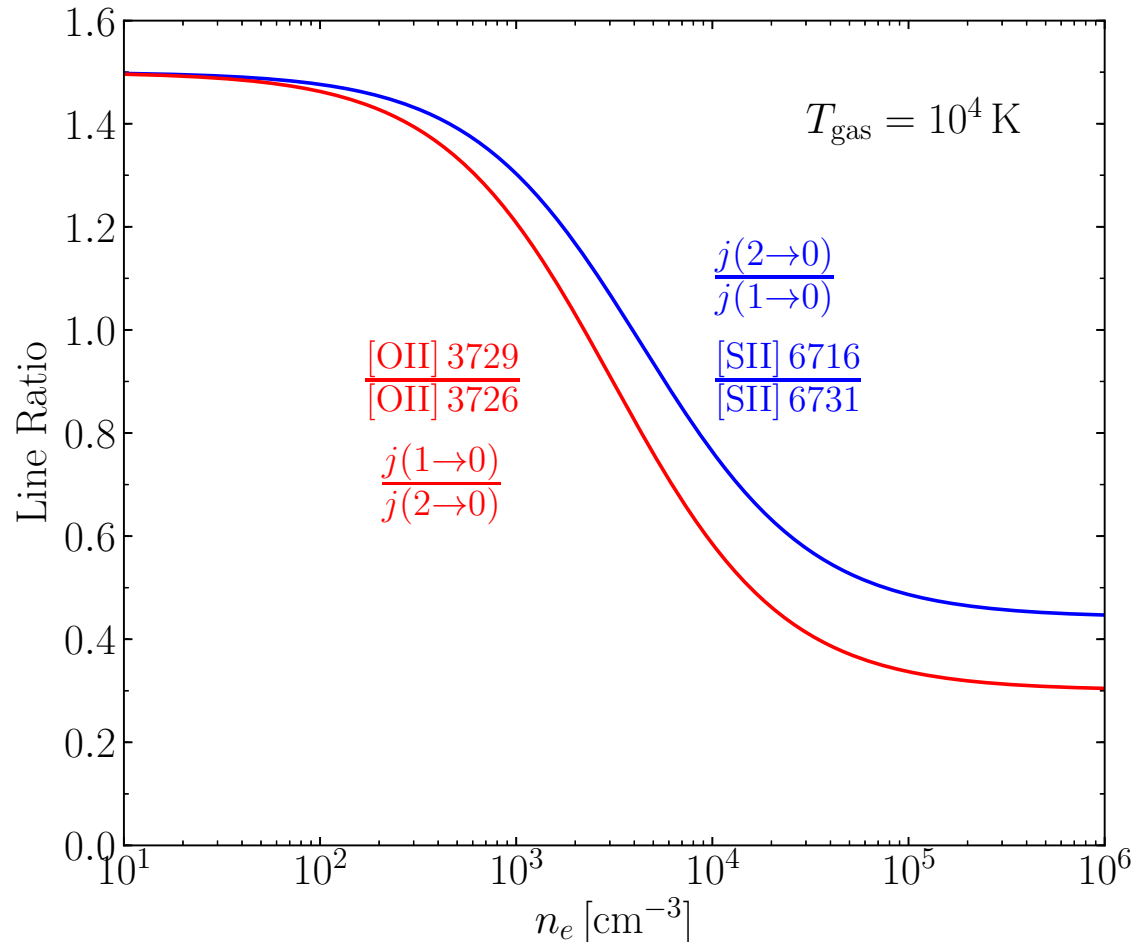
$$g_2 = 6, \quad A_{20} = 2.60 \times 10^{-4} \text{ s}^{-1}$$

$$g_1 = 4, \quad A_{10} = 8.82 \times 10^{-4} \text{ s}^{-1}$$

$$\frac{j(6716)}{j(6731)} = 1.5 \frac{1 + (n_e / 1.48 \times 10^4 \text{ cm}^{-3}) T_4^{-1/2}}{1 + (n_e / 4.37 \times 10^3 \text{ cm}^{-3}) T_4^{-1/2}}$$

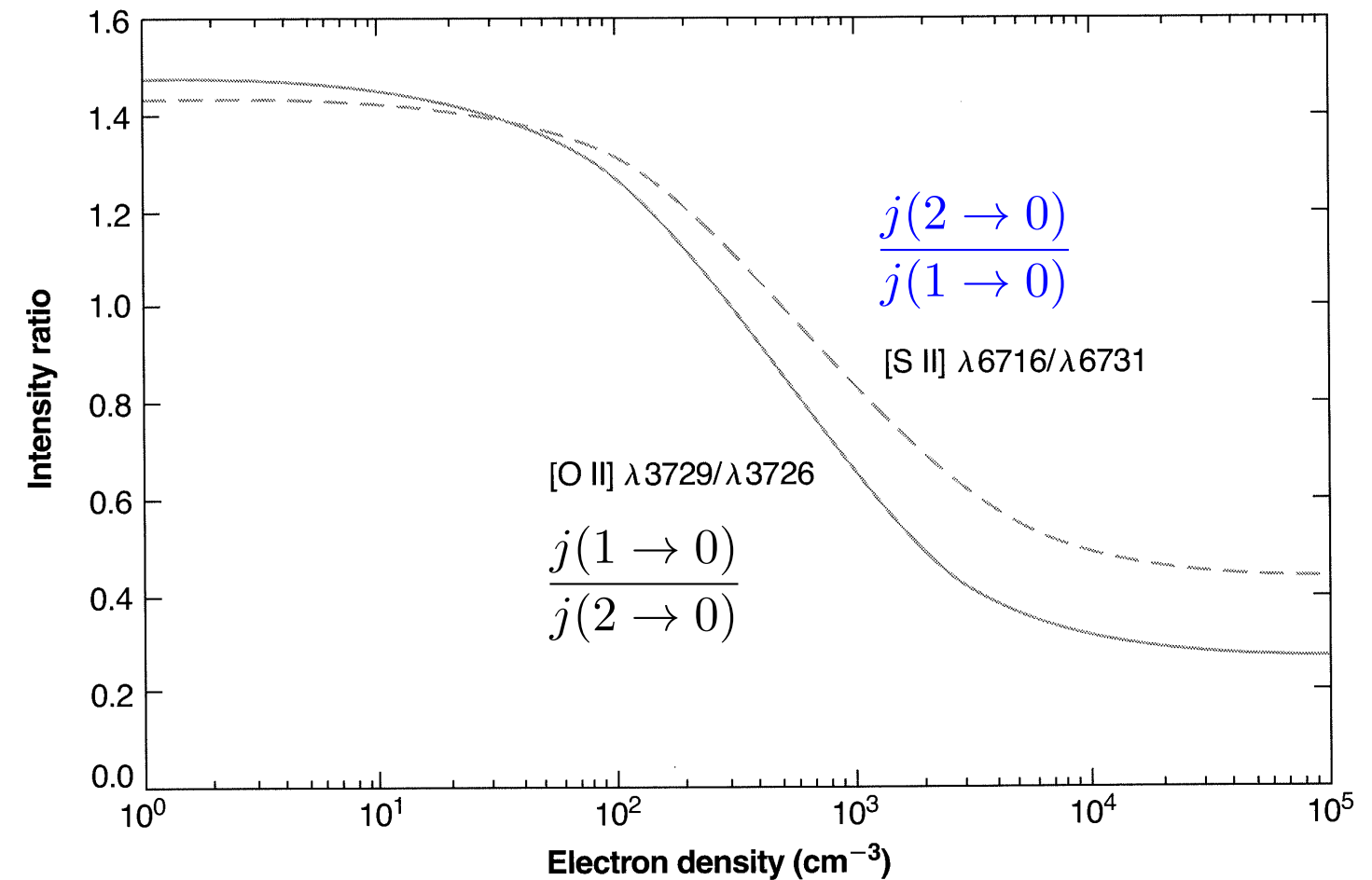
$$\langle \Omega_{20} \rangle = 6.90 \times (6/10)$$

$$\langle \Omega_{10} \rangle = 6.90 \times (4/10)$$



Obtained using the approximate equations in this lecture note.

Note differences between two figures.



The full solution of the equilibrium equations, which also takes into account all transitions, including excitation to the ${}^2\text{P}^\circ$ levels with subsequent cascading downward.

Figure 5.8 [Osterbrock]

Abundance Determination

- He abundance
 - The abundance of He is determined from comparison of the strengths of radiative recombination lines of H and He in regions ionized by stars that are sufficiently hot ($T_{\text{eff}} \gtrsim 3.9 \times 10^4 \text{ K}$) so that He is ionized throughout the H II regions.
- Heavy elements
 - can be inferred by comparing the strengths of collisionally excited lines with recombination lines of H.
 - **Oxygen:**

$$4\pi j([\text{OIII}] 5008) = n_e n(\text{O}^{+2}) k_{03} \frac{A_{32}}{A_{31} + A_{32}} E_{32}$$

$$4\pi j(\text{H}\beta) = n_e n(\text{H}^+) \alpha_{\text{eff}, \text{H}\beta} E_{\text{H}\beta}$$

where

$$\alpha_{\text{eff}, \text{H}\beta} \approx 3.03 \times 10^{-14} T_4^{-0.874 - 0.058 \ln T_4} \text{ cm}^3 \text{ s}^{-1}$$

$$k_{03} = 8.62942 \times 10^{-8} T_4^{-1/2} \frac{\Omega_{30}}{g_0} e^{-E_{30}/kT} \text{ cm}^3 \text{ s}^{-1} \quad (g_0 = 1)$$

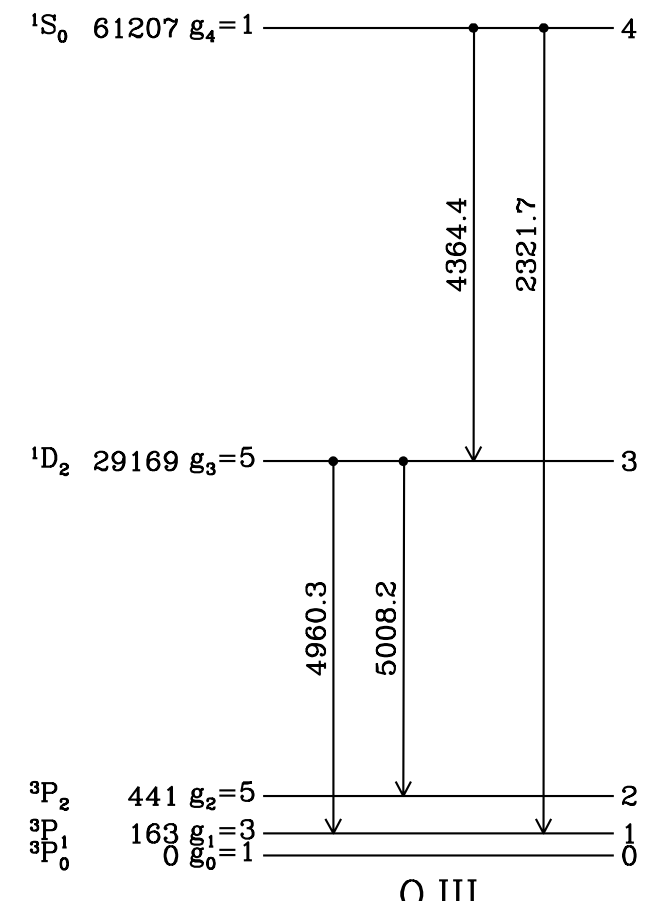
$$E_{32}/k = 29169 \text{ K}, \quad E_{\text{H}\beta}/k = 29588.5 \text{ K}$$

$$\Omega_{30} = 0.243 T_4^{0.120 + 0.031 \ln T_4}$$

$$A_{32} = 2.0 \times 10^{-2} \text{ [s}^{-1}\text{]}$$

$$A_{31} = 6.8 \times 10^{-3} \text{ [s}^{-1}\text{]}$$

$$\frac{[\text{O III}] 5008}{\text{H}\beta} = 5.091 \times 10^5 T_4^{0.494 + 0.089 \ln T_4} e^{-2.917/T_4} \frac{n(\text{O}^{+2})}{n(\text{H}^+)}$$



- **Nitrogen:**

$$4\pi j(\text{[NII]} 6585) = n_e n(\text{N}^+) k_{03} \frac{A_{32}}{A_{31} + A_{32}} E_{32}$$

$$4\pi j(\text{H}\alpha) = n_e n(\text{H}^+) \alpha_{\text{eff}, \text{H}\alpha} E_{\text{H}\alpha}$$

where

$$\alpha_{\text{eff}, \text{H}\alpha} \approx 1.17 \times 10^{-13} T_4^{-0.942 - 0.031 \ln T_4} \text{ cm}^3 \text{ s}^{-1}$$

$$k_{03} = 8.62942 \times 10^{-8} T_4^{-1/2} \frac{\Omega_{30}}{g_0} e^{-E_{30}/kT} \text{ cm}^3 \text{ s}^{-1} \quad (g_0 = 1)$$

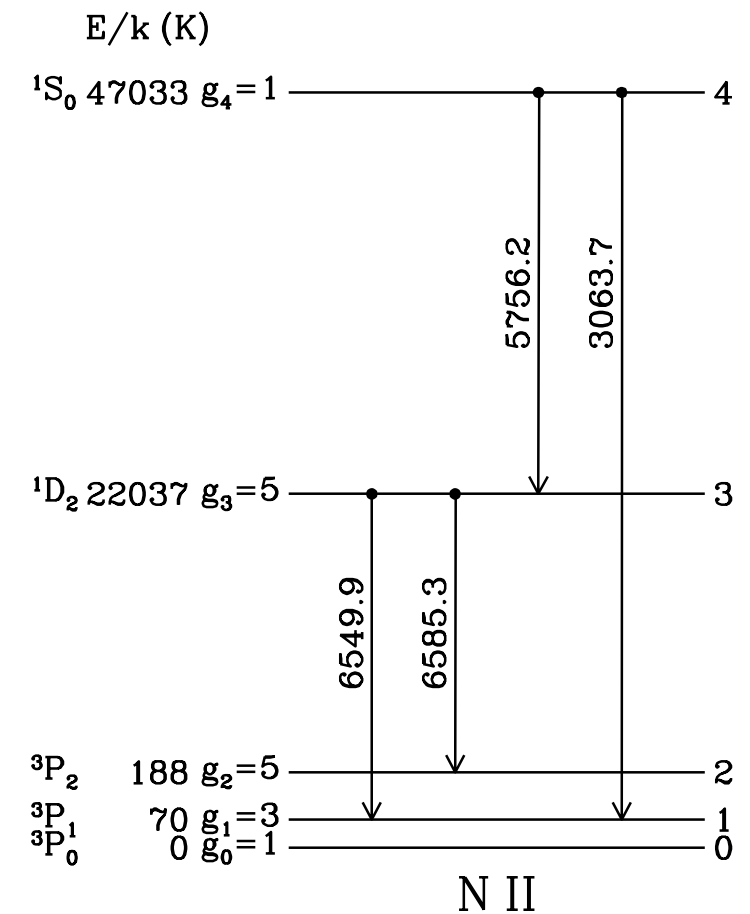
$$E_{32}/k = 21849 \text{ K}, \quad E_{\text{H}\alpha}/k = 21916.9 \text{ K}$$

$$\Omega_{30} = 0.303 T_4^{0.053 + 0.009 \ln T_4}$$

$$A_{32} = 3.0 \times 10^{-3} \text{ [s}^{-1}]$$

$$A_{31} = 9.8 \times 10^{-4} \text{ [s}^{-1}]$$

$$\frac{[\text{NII}]\ 6585}{\text{H}\alpha} = 1.679 \times 10^5 T_4^{0.495 + 0.040 \ln T_4} e^{-2.185/T_4} \frac{n(\text{N}^+)}{n(\text{H}^+)}$$



- Therefore, if the temperature T is known, the relative abundance of the ion can be obtained from the measured line ratio.
- The total elemental abundances are then obtained by applying ***ionization correction factors (ICFs)***, which correct for abundances of unobserved ions.

General Multilevel Atom

- It is easy to generalize the equations of statistical equilibrium up to an arbitrary number of levels.
 - In equilibrium, the rate of collisional and radiative population of any level j is matched by the collisional and radiative depopulation rates of that same level.
 - When combined with the population normalization equation (the sum of the populations of all levels must add up to the total number of ions), we have a linear set of simultaneous equations which may be solved in the standard way.

$$\sum_{i \neq j}^M n_i n_e k_{ij} + \sum_{i=j+1}^M n_i A_{ij} - n_j \left(\sum_{i \neq j}^M n_e k_{ji} + \sum_{i=1}^{j-1} A_{ji} \right) = 0 \quad j = 1, 2, 3, \dots, M$$

$$\sum_{j=0}^M n_j = 1 \quad (\text{normalization}) \quad M + 1 \equiv \text{number of levels}$$

Useful softwares to calculate line ratios.

(1) PopRatio: <http://www.ignacioalex.com/popratio/>
Silva & Viegas (2001, Computer Physics Communications, 136, 319)

(2) PyNeb: <http://research.iac.es/proyecto/PyNeb/>; https://github.com/Morisset/PyNeb_devel
Luridiana, Morisset, & Shaw (2015, A&A, 573, A42)

Ionization / Excitation Diagnostics: The BPT diagram

- Ionization / Excitation Mechanisms in galaxies
 - The optical line emission from star-forming galaxies is usually dominated by emission lines from H II regions.
 - Some galaxies have strong continuum and line emission from an active galactic nucleus (AGN). The line emission is thought to come from gas that is heated and ionized by X-rays from the AGN.
 - ▶ **Seyfert galaxies:** The AGN spectrum normally includes strong emission lines from high-ionization species like C IV and Ne V, which are presumed to be ionized by X-rays from the AGN. Seyfert (1943) discovered that some galaxies had extremely luminous, point-like nuclei, with emission line widths in some cases exceeding 4000 km/s.
 - ▶ **LINEARs** (Low Ionization Nuclear Emission Region): In other cases, the nucleus has strong emission lines but primarily from low-ionization species.
- BPT diagram:
 - Baldwin, Phillips & Terlevich (1981) found that one could distinguish star-forming galaxies from galaxies with spectra dominated by AGNs by plotting the ratio of $[\text{OIII}]5008/\text{H}\beta$ vs. $[\text{NII}]6585/\text{H}\alpha$.
 - These lines are among the strongest optical emission lines from H II regions.
 - The line ratios employ pairs of lines with similar wavelengths so that the line ratios are nearly unaffected by dust extinction.

-
- Recall the structure of H and He ionization zone:
 - In H II regions where He is neutral (no photons with $E > 24.6 \text{ eV}$), N and O will be essentially 100% singly ionized throughout the H ionization zone.
 - On the other hand, for O stars that are hot enough ($24.6 < E < 54.6 \text{ eV}$) to have an appreciable zone of He ionization, the N and O in this zone can be doubly ionized.
 - Because N and O have similar second ionization potentials (29.6 and 35.1 eV for N and O, respectively), to a good approximation, HII regions will have:

$$\text{N}^+/\text{N} \approx \text{O}^+/\text{O} \quad \text{and} \quad \text{N}^{+2}/\text{N} \approx \text{O}^{2+}/\text{O}$$

- Essentially all of the gas-phase O and N in the H II region will be either singly or doubly ionized. H will fully ionized in the H II region:

$$n(\text{N}) = n(\text{N}^+) + n(\text{N}^{+2}), \quad n(\text{O}) = n(\text{O}^+) + n(\text{O}^{+2}), \quad \text{and} \quad n(\text{H}) = n(\text{H}^+)$$

- Let's define the fraction of doubly-ionized ion.

$$\xi_{\text{N}} \equiv \frac{n(\text{N}^{+2})}{n(\text{N}^+) + n(\text{N}^{+2})} = \frac{n(\text{N}^{+2})}{n(\text{N})}$$

$$\xi_{\text{O}} \equiv \frac{n(\text{O}^{+2})}{n(\text{O}^+) + n(\text{O}^{+2})} = \frac{n(\text{O}^{+2})}{n(\text{O})}$$

$$\xi_{\text{N}} \approx \xi_{\text{O}} \implies \xi$$

- We assume the N abundance to be solar, and the O abundance to be 80% solar (20% is presumed to be in silicate grains).
- In terms of the fraction,

$$\frac{n(\text{N}^+)}{n(\text{H}^+)} = (1 - \xi) \frac{n(\text{N})}{n(\text{H})} \quad \frac{n(\text{O}^{2+})}{n(\text{H}^+)} = \xi \frac{n(\text{O})}{n(\text{H})}$$

- Then, the line ratios can be written:

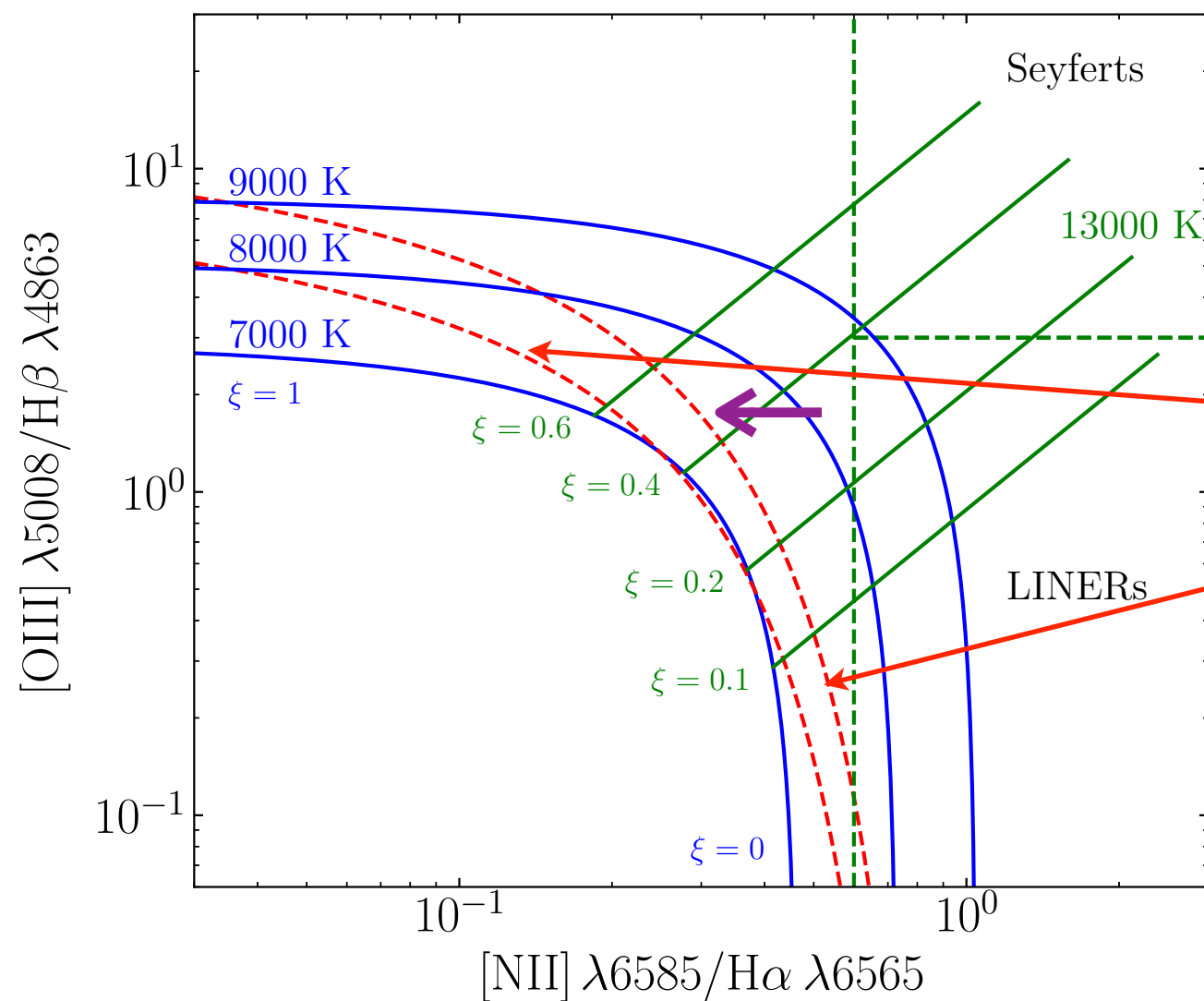
$$\frac{[\text{O III}] 5008}{\text{H}\beta} = 218.7 \xi T_4^{0.494 + 0.089 \ln T_4} e^{-2.917/T_4} \left(\frac{n_{\text{O}}/n_{\text{H}}}{0.8 \times 5.37 \times 10^{-4}} \right)$$

$$\frac{[\text{N II}] 6585}{\text{H}\alpha} = 12.44 (1 - \xi) T_4^{0.495 + 0.040 \ln T_4} e^{-2.185/T_4} \left(\frac{n_{\text{N}}/n_{\text{H}}}{7.41 \times 10^{-5}} \right)$$

- Then, for an assumed temperature T, we can produce a theoretical curve of [OIII]5008/H β versus [NII]6585/H α by varying the fraction ξ of the N and O that is doubly ionized.

The theoretical curve of [OIII]5008/H β versus [NII]6585/H α that is obtained by varying the fraction is shown below:

Blue dashed lines show the tracks of the equations calculated, by varying ξ from 0 to 1, for $T = 7000, 8000$, and 9000 K.



Empirical curves that discriminate the star-forming galaxies from AGNs.

$$\log_{10} ([\text{OIII}]/\text{H}\beta) = 1.10 - \frac{0.60}{0.01 - \log_{10} ([\text{NII}]/\text{H}\beta)}$$

$$\log_{10} ([\text{OIII}]/\text{H}\beta) = 1.3 - \frac{0.61}{0.05 - \log_{10} ([\text{NII}]/\text{H}\beta)}$$

Kauffmann et al. (2003, MNRAS, 346, 1055)

To derive the equation, we assumed that $\xi_N = \xi_O = \xi$. The discrepancy between the simple model with the observations would be due to the assumption. We need to note that $E(\text{N}^+ \rightarrow \text{N}^{2+}) < E(\text{O}^+ \rightarrow \text{O}^{2+})$, which implies that $\xi_N \gtrsim \xi_O$.

The arrow ← indicates the direction that is expected from $\xi_N > \xi_O$.

- Line ratios for 122514 galaxies in SDSS DR7 with S/N > 5.

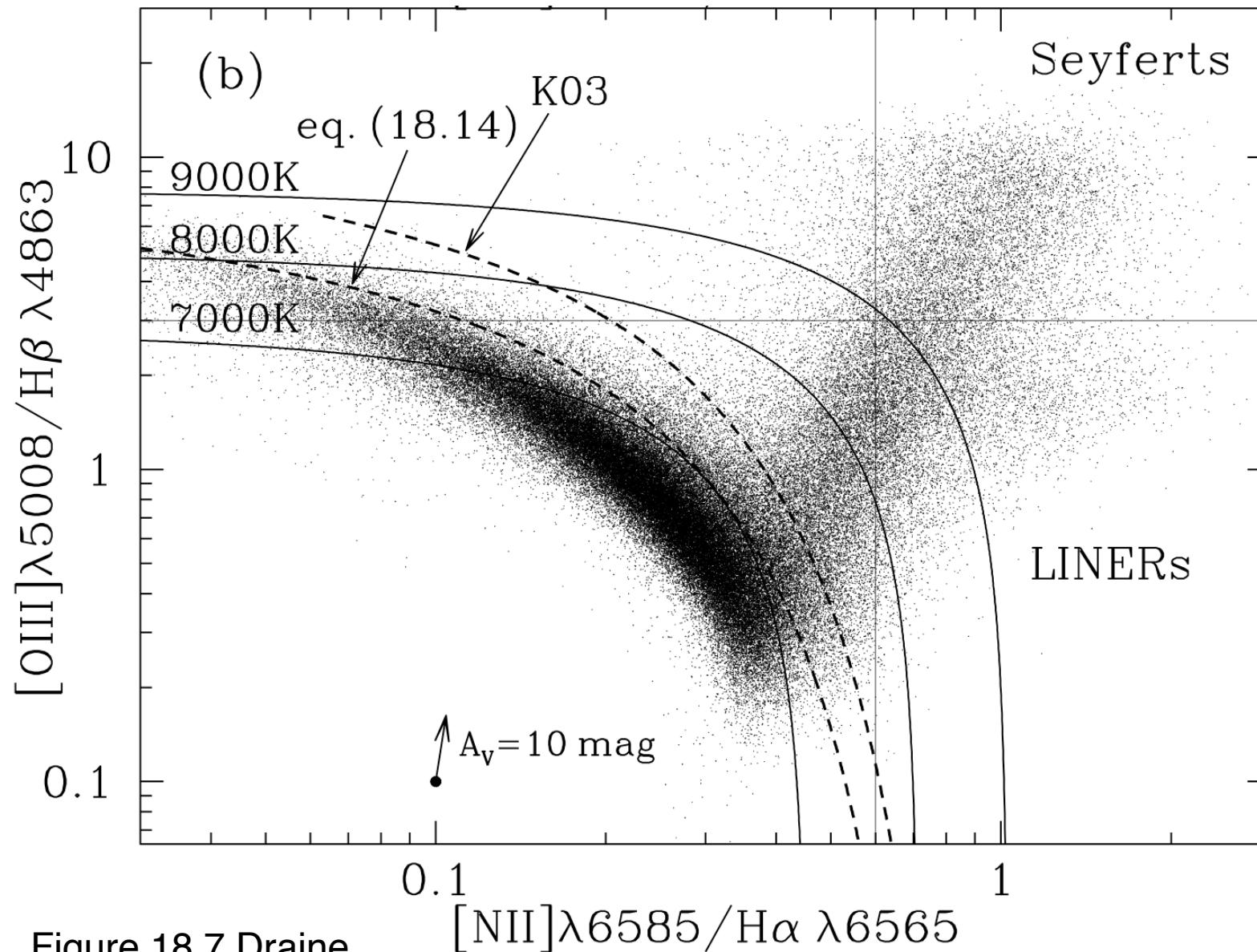


Figure 18.7 Draine



Flying seagull [Stasinska]

Photons from AGNs are harder than those from the massive stars that power H II regions.
They induce more heating, implying that optical collisionally excited lines will be brighter with respect to recombination lines than in the case of ionization by massive stars.
The heating by an AGN boosts the [N II] line and creates a clear separation of the two wings.

Dynamics of H II regions

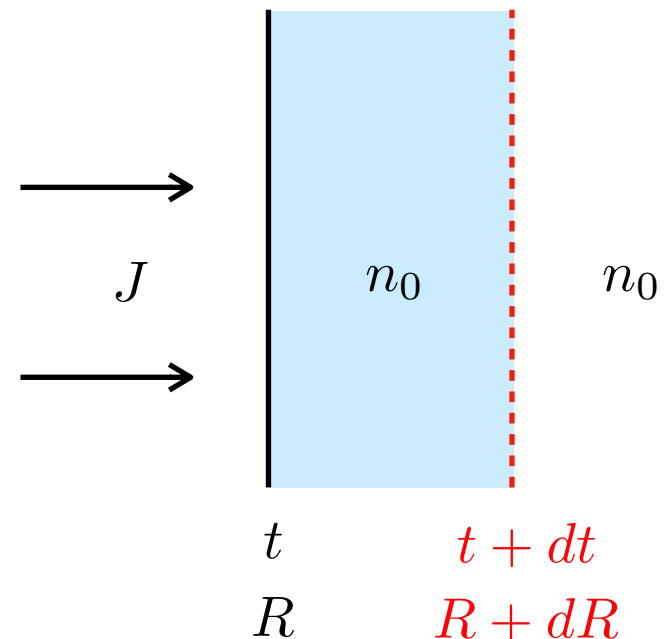
- A new O star is presumably born within clouds of relatively dense cold gas. The appearance of a source of UV photons will have two effects.
 - First, the gas surrounding the new star will become ionized. Since the mean free path of an UV photon is very short in neutral hydrogen, the photons will be absorbed in a relatively thin surrounding shell of neutral hydrogen, producing new ionization. Thus the ionized and neutral gases are separated by an ionization front, which moves rapidly outward as more and more atoms become ionized by the stream of photons.
 - Second, the process increases the gas temperature from $\sim 10^2$ K to $\sim 10^4$ K, by a factor of about a hundred. the ionization process itself increases the number of gas particles, by a factor two. As a result, ***the pressure in the ionized gas is ~200 times greater than that in surrounding neutral material.*** This ionized gas cannot be confined and will expand. The ionized and neutral gas are set in motion.
 - Since the expansion velocity is likely to exceed the sound velocity in the surrounding H I region, a shock front may be expected to form, moving out through the neutral gas. The dynamical analysis of H II regions must consider the interactions between the ionization front and the shock front, together with the equations of motion of the gas behind the two fronts.
- This process is not the only way in which ISM is set in motion by means of interaction with stars.
 - There are effects produced by the very high speed continuous mass loss - a stellar wind.
 - Many massive stars terminate their existence in a violent explosive event - a supernova.

-
- Basic Assumptions:
 - Any disturbances to the cloud structure produced by the formation of a star are neglected. After a relatively short time ($< 10^5$ yr), the star reaches a static configuration in which it can remain for a much longer time ($> 3 \times 10^6$ yr). The stellar radiant energy output rate and the spectral distribution of the radiation are more or less constant during this phase. The star then produces Lyman continuum photons at a constant rate. Since the star formation time scale is so short, we may take the star to be ‘switched on’ instantaneously.
 - The gas around the star will be assumed to be at rest (in the frame of reference of the star).
 - The gas has initially assumed to be uniform in density and temperature.
 - Ionization front
 - The term “front” describes a more-or-less abrupt boundary between two regions of the ISM with very different properties.
 - An ionized nebula can be approximated as a region of highly ionized gas, separated from the surrounding neutral medium by a thin boundary region, of thickness $\lambda_{\text{mfp}} \sim 0.002 \text{ pc}$. Thus, an H II region is surrounded by an ionization front.

The velocity of the ionization front

- Suppose that at time t the ionization front is located at a distance R from the star and at time $t + dt$ it is at a distance $R + dR$.

- Let n_0 = number density of the undisturbed neutral hydrogen
 - J = number of Lyman continuum photons incident normally on unit area of the ionization front per unit time.



- Ionization balance: While the ionization front moves from R to $R + dR$, the photons will ionize all the neutral atoms lying between these two positions $(R, R + dR)$.
 - We assume that only one photon is needed to ionize each atom as the front moves the distance dR . In other words, no recombination occurs within the distance interval dR . For unit area of the ionization front, the following relation must be satisfied:

$$Jdt = n_0 dR$$

- Then, the velocity of the ionization front (in a fixed frame of reference) is:

$$\frac{dR}{dt} = \frac{J}{n_0}$$

The Radius of the Ionization Front: initial stage

- Suppose that the UV source has been suddenly turned on.
 - Ionization balance equation: We consider two factors:
 - ▶ The radiation field at the ionization front is diluted because of the spherical geometry.
 - ▶ Recombination takes place continuously inside the ionized region, and some of the UV photons produced by the central source must go to reionize the atoms that have recombined.
- Inside the ionized sphere, the fractional ionization is near unity. Thus, $n_e = n_p = n_0$. Using this condition, we obtain an equation for the velocity of the ionization front.

$$\frac{J}{n_H} = \frac{dR}{dt} = \frac{Q_0}{4\pi R^2 n_0} - \frac{1}{3} R n_0 \alpha_B$$

- Now, define the following dimensionless quantities:

$$\rho \equiv R/R_s \quad \text{where } Q_0 \equiv \left(\frac{3}{4\pi} \frac{Q_0}{\alpha_B n_0^2} \right)^{1/3}$$

$$\tau \equiv t/t_{\text{rec}} \quad \text{where } t_{\text{rec}} \equiv \frac{1}{\alpha_B n_0}$$

Then, the equation in dimensionless form is

$$\frac{d\rho}{d\tau} = \frac{1}{3} \left(\frac{1}{\rho^2} - \rho \right)$$

- The equation can be written:

$$\frac{d\rho}{d\tau} = \frac{1}{3} \left(\frac{1}{\rho^2} - \rho \right) \rightarrow \frac{d\rho^3}{d\tau} = 1 - \rho^3$$

- It's solution is

$$\rho^3 = 1 - e^{-\tau}$$

$$R(t) = R_s \left(1 - e^{-t/t_{\text{rec}}} \right)^{1/3}$$

$$\begin{aligned} \frac{dx}{d\tau} + x &= 1 \\ e^\tau \frac{dx}{d\tau} + e^\tau x &= e^\tau \\ \frac{d(e^\tau x)}{d\tau} &= e^\tau \end{aligned} \quad \boxed{\rightarrow e^\tau x = \int_0^\tau e^{\tau'} d\tau' = e^\tau - 1} \quad x = 1 - e^{-\tau}$$

- Scale Parameters:

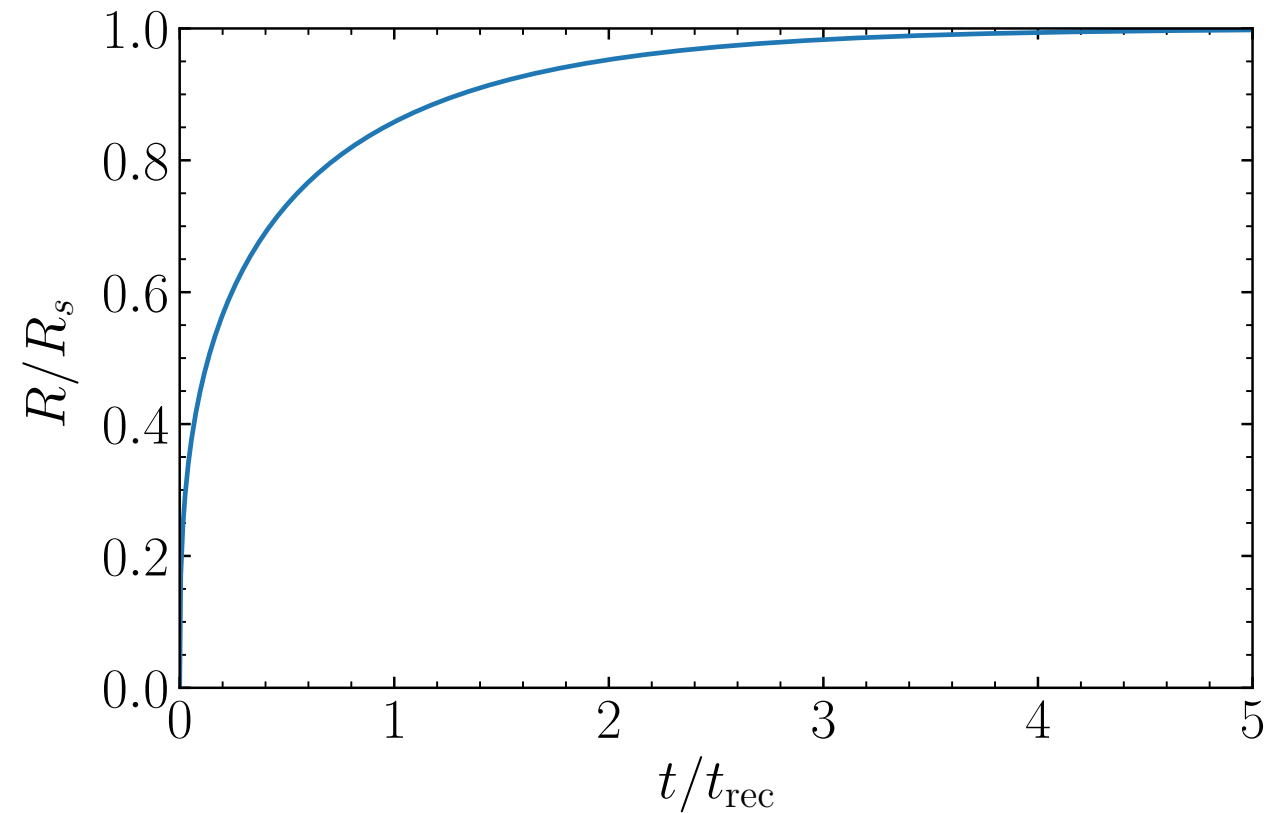
- The time scale introduced is the recombination time scale:

$$t_{\text{rec}} \equiv \frac{1}{\alpha_B n_0} \approx 4000 \text{ yr} \left(\frac{\alpha_B}{2.6 \times 10^{-3} \text{ cm}^3 \text{ s}^{-1}} \right)^{-1} \left(\frac{n_0}{30 \text{ cm}^{-3}} \right)^{-1}$$

the length scale introduced is the Strömgren radius:

$$R_s \equiv \left(\frac{3}{4\pi} \frac{Q_0}{\alpha_B n_0^2} \right)^{1/3} \approx 7 \text{ pc} \left(\frac{Q_0}{10^{49} \text{ s}^{-1}} \right)^{1/3} \left(\frac{\alpha_B}{2.6 \times 10^{-3} \text{ cm}^3 \text{ s}^{-1}} \right)^{-1/3} \left(\frac{n_0}{30 \text{ cm}^{-3}} \right)^{-2/3}$$

-
- Hence, the time required to create a Strömgren sphere after turning on a hot star is ~ 4000 yr. This is also the time it takes the Strömgren sphere to revert to neutral hydrogen after the central UV source has been turned off.



- At times $t \gg t_{\text{rec}} \sim 4000$ yr , the gas medium will be fully ionized with radius $R \sim R_s \sim 7$ pc, surrounded by a partially ionized boundary of thickness $\sim \lambda_{\text{mfp}} = (n_{\text{H}}\sigma_{\text{pi}})^{-1} \sim 0.002$ pc $\ll R_s$.

- We can compute the rate of expansion of the ionization front:

$$\frac{dR}{dt} = \frac{R_s}{3t_{\text{rec}}} \frac{e^{-t/t_{\text{rec}}}}{(1 - e^{-t/t_{\text{rec}}})^{2/3}}$$

where the characteristic expansion velocity is

$$v_* \equiv \frac{R_s}{3t_{\text{rec}}} \simeq 560 \text{ km s}^{-1} \left(\frac{Q_0}{10^{49} \text{ s}^{-1}} \right)^{1/3} \left(\frac{n_0}{30 \text{ cm}^{-3}} \right)^{1/3}$$

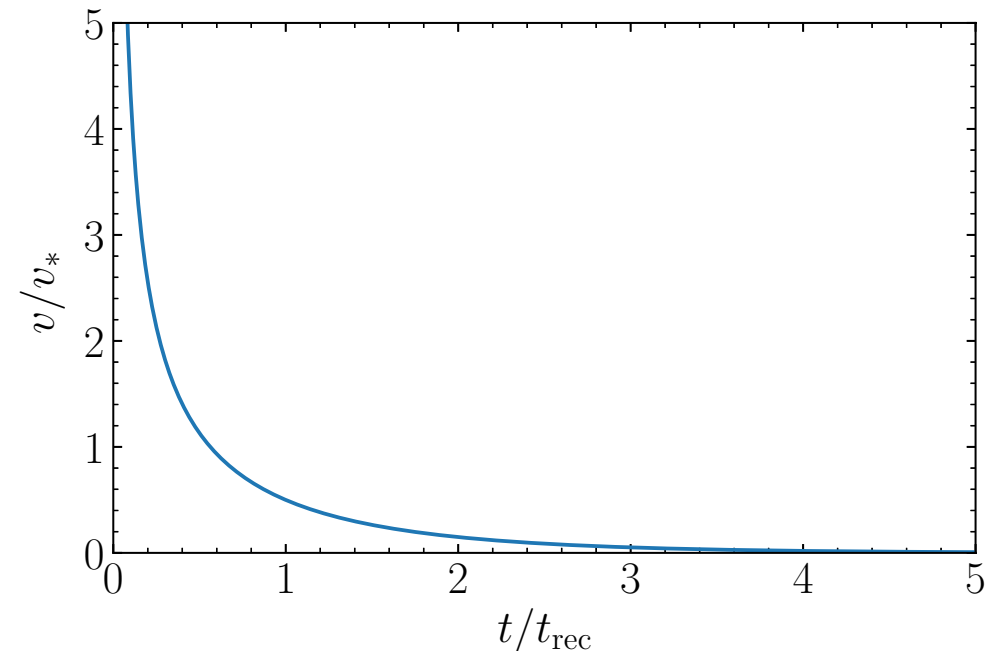
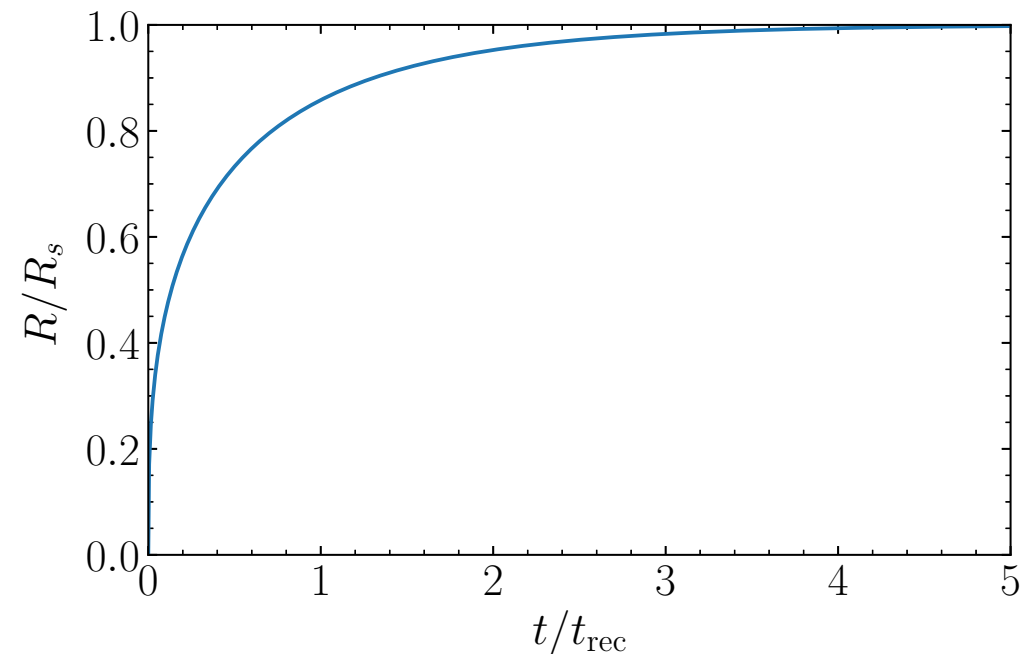
This is much larger than the sonic speed $c_s \approx 1 \text{ km s}^{-1}$ in the neutral medium and $c_s \approx 10 \text{ km s}^{-1}$.

- The expansion speed of the ionization front at two limits:

$$\frac{dR}{dt} \approx \frac{R_s}{3t_{\text{rec}}} \left(\frac{t}{t_{\text{rec}}} \right)^{-2/3} \quad \text{for } t \ll t_{\text{rec}}$$

$$\frac{dR}{dt} \approx \frac{R_s}{3t_{\text{rec}}} e^{-t/t_{\text{rec}}} \quad \text{for } t \gg t_{\text{rec}}$$

Note that the expansion speed diverges at $t = 0$.



-
- The ionization front will initially expand supersonically. When will the ionization front expand at subsonic speeds?

$$\frac{dR}{dt} = \frac{R_s}{3t_{\text{rec}}} e^{-t/t_{\text{rec}}} \lesssim c_s$$

$$t \lesssim t_{\text{sonic}} \equiv t_{\text{rec}} \ln \left(\frac{R_s}{3t_{\text{rec}}} \frac{1}{c_s} \right) \approx 3.8t_{\text{rec}} \simeq 15,000 \text{ yr}$$

- At this time, the ionization front will have a size of:

$$R(t = t_{\text{sonic}}) = R_s (1 - e^{-3.8})^{1/3} = 0.9925 R_s$$

- The ionization front will expand at a supersonic velocity until $t \approx t_{\text{sonic}}$ ($\sim 15,000$ yr). By that time, the ionized sphere has reached a radius $R \sim 0.99 R_s$ and then it starts to expand at subsonic speed.
- At $t = R_s/c_s \sim 0.5 \text{ Myr}$, the gas starts to flow outward as a result of the pressure gradient that has build up.

The final stage of evolution of an ionized region

- Although the ionized sphere approaches ionization equilibrium at $t \gtrsim t_{\text{rec}}$, it would be still far from pressure equilibrium.
 - Outside the ionized zone, it will be embedded in the cold neutral medium with a temperature $T \sim 100$ K.
 - Inside the sphere, the heating and cooling processes yield a temperature of $T \sim 10000$ K.
 - Also, the density of particles inside the ionized sphere will double when the hydrogen is ionized.
 - Thus, the pressure inside the sphere will be ~ 200 times higher than the pressure outside, meaning that the ionized gas will begin to expand.
 - The ionized gas expands as long as it has a higher pressure than its surroundings. This expansion produces a shock and will cease when the hot ionized gas reaches pressure equilibrium with the surrounding cold neutral gas.
- The condition of final pressure equilibrium can be written in the form:

$$2n_f k T_i = n_0 k T_n$$

n_f = the ionized gas density.

T_i and T_n = the ionized and neutral gas temperature, typically $T_i = 10^4$ K, $T_n = 10^2$ K.

-
- The ionized gas sphere must still absorb all the stellar UV photons. Thus,

$$Q_0 = \frac{4}{3}\pi R_f^3 n_f^2 \alpha_B$$

Here, R_f is the final radius of the ionized gas sphere. From the pressure equilibrium condition, we obtain the final size:

$$n_f = (T_n/2T_i)n_0 \approx 0.005n_0 \quad \rightarrow \quad R_f = (2T_i/T_n)^{2/3}R_s \approx 34R_s$$

- The ratio of the mass of gas finally ionized to that contained within the initial Stromgren sphere is:

$$\frac{M_f}{M_s} = \frac{R_f^3 n_f}{R_s^3 n_0} = \frac{2T_i}{T_n} \approx 2000$$

- This indicates that the initial Stromgren sphere contains only a very small fraction of the material which, in principle, a star could ultimately ionize.

The intermediate stage of evolution of an ionized region

- Before the pressure equilibrium is established, the gas density and temperature will be

$$n_i \approx 2n_0 < n_f \quad \text{and} \quad T_i = 10^4 \text{ K}$$

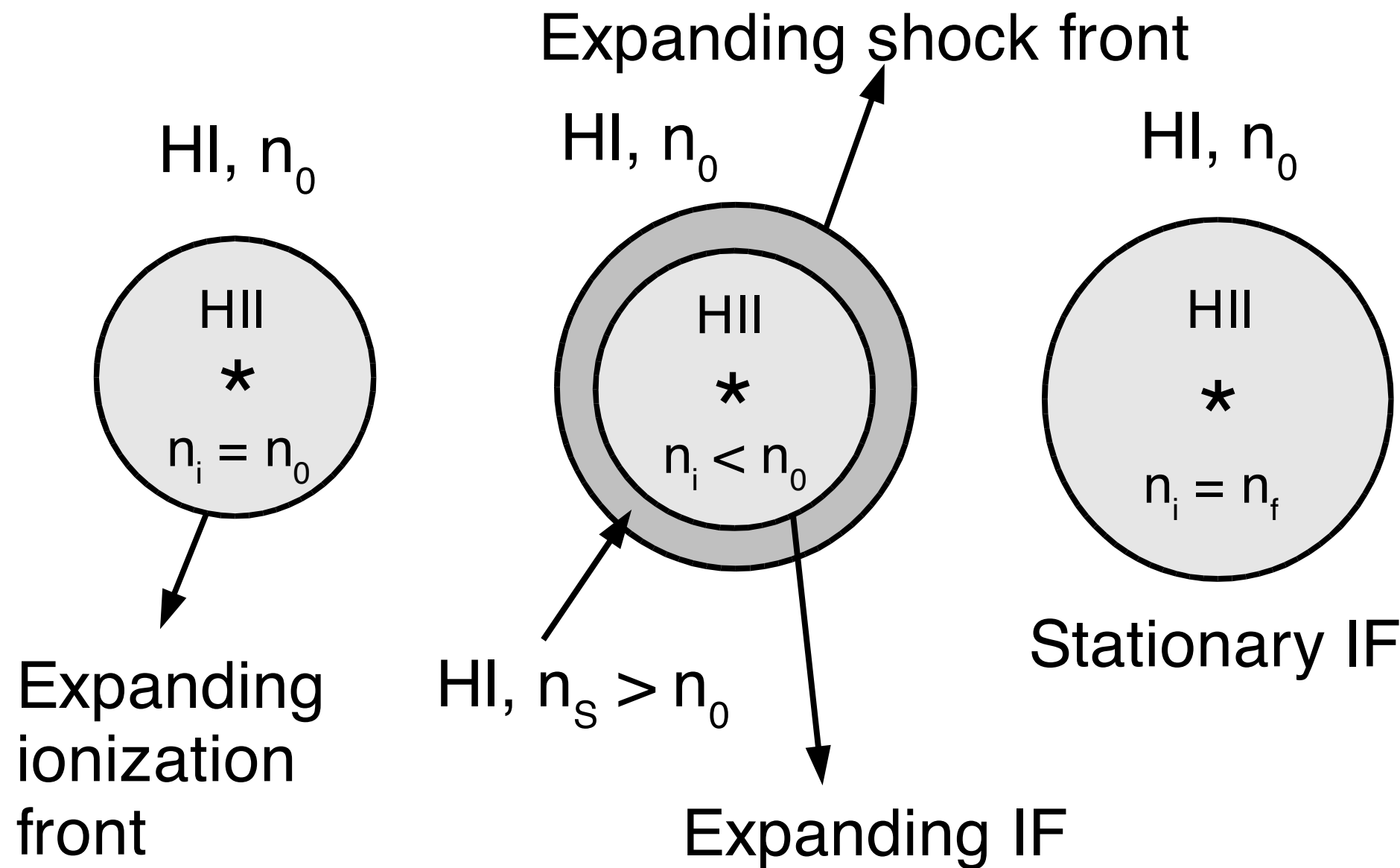
- Then the isothermal sound speeds of the ionized gas and neutral gas are, respectively:

$$c_i^2 = \frac{P_i}{\rho_i} \approx \frac{2n_0 k T_i}{n_0 m_H} \quad c_n^2 = \frac{P_n}{\rho_n} = \frac{n_0 k T_n}{n_0 m_H}$$

$$\frac{c_i}{c_n} = \left(\frac{n_i T_i}{n_0 T_n} \right)^{1/2} \approx \sqrt{200} = 14.14$$

- The sound speed of the ionized gas is much larger than that of the neutral gas.
- The ionized gas has a higher pressure and thus plays the role of a piston and pushes a shock wave into the neutral gas. The expansion speed of the ionized gas is originally equal to about c_i , which is highly supersonic with respect to the sound speed in the neutral gas.
- Note also that, at $t \gtrsim t_{\text{sonic}} \approx 3.8t_{\text{rec}}$, the expansion speed of ionized gas is larger than that of the ionization front.

$$\frac{dR}{dt} \approx c_n \ll c_i \quad \text{at } t \approx t_{\text{sonic}}$$



Evolutionary scheme of an expanding H II region. (a) The initial stage, (b) expansion with a shock in the neutral gas, (c) the final equilibrium state.

[Figure 7.2 Dyson]

-
- Sound crossing time
 - The ionized region will likely be overpressure relative to its surroundings, in which case it will expand on the sound crossing time.
 - The isothermal sound speed in fully ionized hydrogen is

$$c_s = (2kT/m_{\text{H}})^{1/2} = 13(T/10^4 \text{ K})^{1/2} \text{ km s}^{-1} \quad p = (n_{\text{HI}} + n_e)kT = 2n_{\text{H}}kT$$

- The time for a pressure wave to propagate a distance equal to Strömgren radius is

$$t_{\text{sound}} = \frac{R_s}{c_s} \approx 2.39 \times 10^5 \frac{Q_0/10^{49} \text{ s}^{-1}}{(n/10^2 \text{ cm}^{-3})^{2/3}} \text{ [yr]}$$

- This is about a hundred times longer than the recombination time.
- The lifetime of the main sequence star (for instance, O5 star) is only 1 Myr, so the hottest O stars become supernovae before their H II regions have a chance to reach pressure equilibrium with the surrounding ISM.

Ionization Front: Jump Condition

- Low density gas, like that of the ISM, can be treated as an ideal gas, with no viscosity with a pressure given by the ideal gas law:

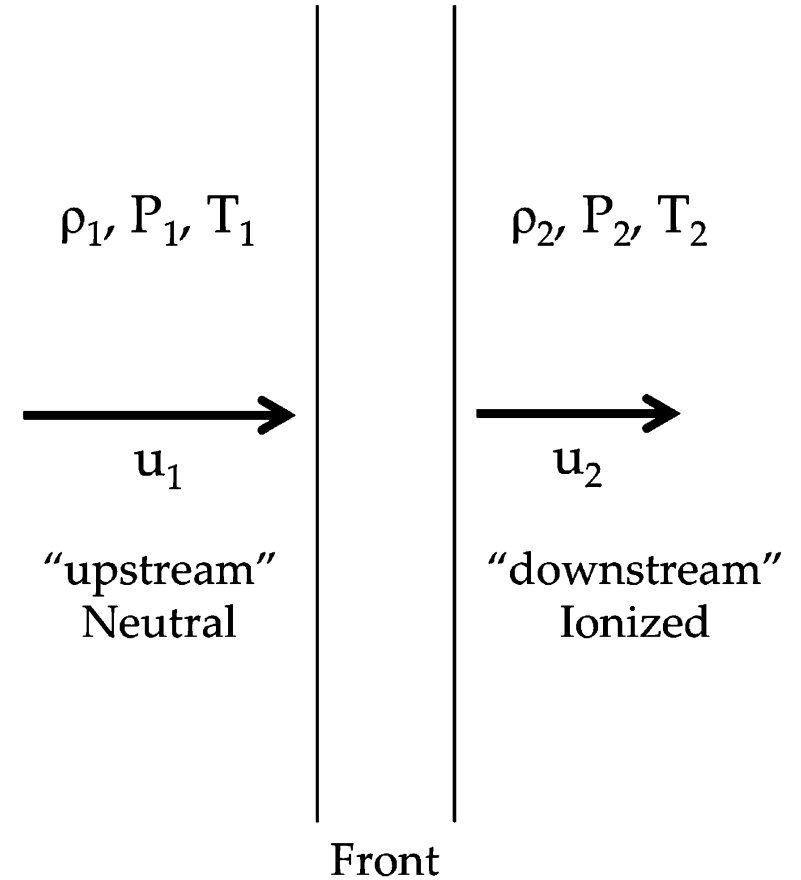
$$P = \frac{\rho k T}{m}$$

ρ = mass density, T = temperature,
 m = mean molecular mass

ρ, P, T, u = density, pressure, temperature, and bulk velocity

- Let's consider a small patch of the ionization front between the interior of an H II region and its exterior.

- If the patch is small compared to the ionization front's radius of curvature, then we can treat the ionization front as if it has **plane parallel** symmetry.
- It is convenient to use **a frame of reference in which the ionization front is stationary**; in this frame, the bulk velocity u_1 of the neutral gas points toward the ionization front. The bulk velocity u_2 of the ionized gas points away from the ionization front.



- Mass conservation

$$\frac{\partial \rho}{\partial t} + \nabla \cdot (\rho \mathbf{u}) = 0$$

$$\frac{\partial \rho}{\partial t} = -\frac{\partial}{\partial x} (\rho u)$$

- This equation says that the density increase is because the flow of gas is converging on that location.

- Momentum conservation

$$\rho \frac{\partial \mathbf{u}}{\partial t} + \rho (\mathbf{u} \cdot \nabla) \mathbf{u} = -\nabla P$$

$$\rho \frac{\partial u}{\partial t} = -\rho u \frac{\partial u}{\partial x} - \frac{\partial P}{\partial x}$$

- We will ignore gravitational and magnetic forces.
- Let's consider a steady state solution.
 - We have seen that the speed of the ionization front surrounding a Stromgren sphere changes with time. However, the steady state solution gives us some intuition about the behavior of ionization fronts in general.
 - Then, the mass conservation and momentum conservation equation becomes:

$$\frac{d}{dx} (\rho u) = 0$$

$$\rho u \frac{du}{dx} + \frac{dP}{dx} = 0$$

-
- The momentum conservation equation is equivalent to

$$\frac{d}{dx} (\rho u^2) - u \frac{d}{dx} (\rho u) + \frac{dP}{dx} = 0$$

- Using the mass conservation equation, the momentum conservation equation becomes:

$$\frac{d}{dx} (\rho u^2 + P) = 0$$

- In summary, we have two equations:

$$\frac{d}{dx} (\rho u) = 0 \quad \frac{d}{dx} (\rho u^2 + P) = 0$$

- Let subscript 1 denote fluid variables in the neutral gas ahead of the I-front, and subscript 2 denotes fluid variables in the ionizing gas behind the I-front. Integrating these equation across the ionization front, we obtain:

$$\rho_1 u_1 = \rho_2 u_2$$

$$\rho_1 u_1^2 + P_1 = \rho_2 u_2^2 + P_2$$

-
- In the mass conservation equation, the mass flow through the front is not arbitrary. Instead, the number of H atoms flowing through the front per unit area per second must equal to J , the corresponding number of ionizing photons reaching the front. Hence, the equation becomes

$$\rho_1 u_1 = \rho_2 u_2 = m_i J$$

Here, $u_1 = \frac{dR}{dt} = \frac{J}{n_0}$, $\rho_1 = m_i n_0$

where m_i is the mean mass of the gas per newly created positive ion ($m_i = m_H$ in a pure hydrogen gas). We may also write the equation of momentum conservation using the isothermal sound speeds:

$$\rho_1 (u_1^2 + c_1^2) = \rho_2 (u_2^2 + c_2^2)$$

- We will consider a hydrogen gas.

$$c_1 = \left(\frac{kT_1}{m_H} \right)^{1/2} = 0.91 \text{ km s}^{-1} \left(\frac{T_1}{100 \text{ K}} \right)^{1/2} \quad \text{neutral hydrogen gas}$$

$$c_2 = \left(\frac{2kT_2}{m_H} \right)^{1/2} = 12.9 \text{ km s}^{-1} \left(\frac{T_2}{10^4 \text{ K}} \right)^{1/2} \quad \text{fully ionized gas}$$

Here, the number density of particles is $2n_H$ in a fully-ionized hydrogen gas (downstream) and thus the factor 2 in c_2 .

- In summary, the equations are

$$\begin{aligned}\rho_1 u_1 &= \rho_2 u_2 = m_i \Psi \\ \rho_1 (u_1^2 + c_1^2) &= \rho_2 (u_2^2 + c_2^2)\end{aligned}$$

- We assume that ρ_1 and u_1 are known, and we seek to solve for the unknown ρ_2 and u_2 . We obtain a simple quadratic equation for $x \equiv \rho_1/\rho_2 = u_2/u_1$.

$$\begin{aligned}\frac{\rho_1}{\rho_2} (u_1^2 + c_1^2) &= \left(\frac{\rho_1}{\rho_2}\right)^2 u_1^2 + c_2^2 \\ u_1^2 x^2 - (u_1^2 + c_1^2) x + c_2^2 &= 0 \quad \longrightarrow \quad x = \frac{1}{2u_1^2} \left[(u_1^2 + c_1^2) \pm \sqrt{(u_1^2 + c_1^2)^2 - 4u_1^2 c_2^2} \right]\end{aligned}$$

- Then, the ratios between densities and velocities are:

$$\frac{u_2}{u_1} = \frac{\rho_1}{\rho_2} = \frac{1}{2u_1^2} \left[(u_1^2 + c_1^2) \pm \sqrt{(u_1^2 + c_1^2)^2 - 4u_1^2 c_2^2} \right]$$

$$\frac{\rho_2}{\rho_1} = \frac{u_1}{u_2} = \frac{1}{2c_2^2} \left[(u_1^2 + c_1^2) \mp \sqrt{(u_1^2 + c_1^2)^2 - 4u_1^2 c_2^2} \right]$$

- The roots are real if and only if

$$\begin{aligned} f(u_1) &\equiv (u_1^2 + c_1^2)^2 - 4u_1^2 c_2^2 \\ &= (u_1^2 + c_1^2 + 2u_1 c_2)(u_1^2 + c_1^2 - 2u_1 c_2) \geq 0 \end{aligned}$$

- This requires:

$$\begin{aligned} u_1^2 + c_1^2 - 2u_1 c_2 &\geq 0 \\ \left[u_1 - \left(c_2 + \sqrt{c_2^2 - c_1^2} \right) \right] \left[u_1 - \left(c_2 - \sqrt{c_2^2 - c_1^2} \right) \right] &\geq 0 \end{aligned}$$

Therefore,

$$u_1 \geq u_R \equiv c_2 + \sqrt{c_2^2 - c_1^2} \quad \text{or} \quad u_1 \leq u_D \equiv c_2 - \sqrt{c_2^2 - c_1^2}$$

We also note that

$$\begin{aligned} u_1^2 + c_1^2 + 2u_1 c_2 &= \left[u_1 + \left(c_2 + \sqrt{c_2^2 - c_1^2} \right) \right] \left[u_1 + \left(c_2 - \sqrt{c_2^2 - c_1^2} \right) \right] \\ \rightarrow \quad f(u_1) &= (u_1^2 - u_R^2)(u_1^2 - u_D^2) \end{aligned}$$

$$\begin{aligned} \frac{u_2}{u_1} &= \frac{\rho_1}{\rho_2} = \frac{1}{2u_1^2} \left[(u_1^2 + c_1^2) \pm \sqrt{(u_1^2 - u_R^2)(u_1^2 - u_D^2)} \right] \\ \frac{\rho_2}{\rho_1} &= \frac{u_1}{u_2} = \frac{1}{2c_2^2} \left[(u_1^2 + c_1^2) \mp \sqrt{(u_1^2 - u_R^2)(u_1^2 - u_D^2)} \right] \end{aligned}$$

- The rapidly propagating ionization fronts, with $u_1 \geq v_R$ are called ***R-type fronts (R stands for “rarefied” or rapid)***. The dilatory ionization fronts are called ***D-type fronts (D stands for “dense” or dilatory)***.
- An R-type front has $u_1 \geq u_R > c_2 > c_1$, and is supersonic with respect to the neutral medium.
- A D-type front has $u_1 \leq u_D < c_1 < c_2$, and is subsonic with respect to the neutral medium.
- For a given front propagation speed u_1 , there are two possible values of the density ratio ρ_2/ρ_1 across the ionization front as a function of the propagation speed u_1 .
 - ▶ The front that has the ***larger density contrast*** is called a ***strong*** front.
 - ▶ The front that has the ***smaller density contrast*** is called a ***weak*** front.
 - ▶ Thus, there are four types of ionization front: weak R, strong R, weak D, strong D.

$$\frac{\rho_2}{\rho_1} = \frac{1}{2c_2^2} \left[(u_1^2 + c_1^2) \pm \sqrt{(u_1^2 - u_R^2)(u_1^2 - u_D^2)} \right]$$

R-front: $u_1 \geq u_R$ weak –; strong +
 D-front: $u_1 \leq u_D$ weak +; strong –

- ▶ The solutions for $u_1 = u_R$ and $u_1 = u_D$ are called “R-critical” and “D-critical”, respectively.

- Since c_2 exceeds c_1 by about one or two order of magnitude in an interstellar ionization front ($c_2 \gg c_1$),

$$u_R = c_2 + \sqrt{c_2^2 - c_1^2} \approx c_2 + c_2 \left(1 - \frac{1}{2} \frac{c_1^2}{c_2^2} - \frac{1}{8} \frac{c_1^4}{c_2^4} \right)$$

$$u_D = c_2 - \sqrt{c_2^2 - c_1^2} \approx c_2 - c_2 \left(1 - \frac{1}{2} \frac{c_1^2}{c_2^2} - \frac{1}{8} \frac{c_1^4}{c_2^4} \right)$$

$$u_R \approx 2c_2 \left(1 - \frac{1}{4} \frac{c_1^2}{c_2^2} \right) > c_2 > c_1 > u_D$$

$$u_D \approx \frac{1}{2} \frac{c_1^2}{c_2} \left(1 + \frac{1}{4} \frac{c_1^2}{c_2^2} \right) < c_1 < c_2 < u_R$$

- Approximate solutions:

R-critical $\frac{\rho_2}{\rho_1} \approx 2 \left(1 - \frac{1}{4} \frac{c_1^2}{c_2^2} \right)$ for $u_1 = u_R$

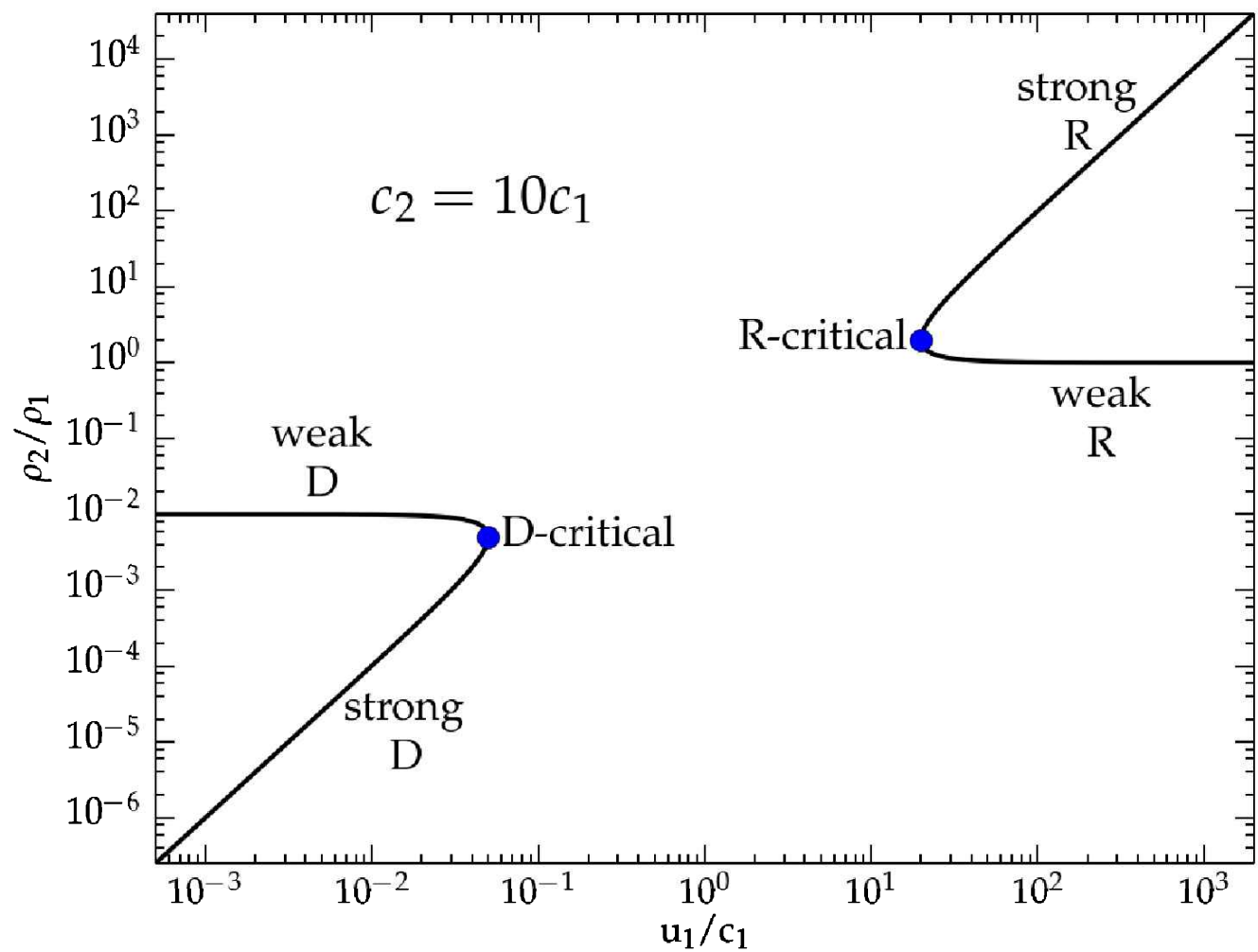
D-critical $\frac{\rho_2}{\rho_1} \approx \frac{1}{2} \frac{c_1^2}{c_2^2} \left(1 + \frac{1}{4} \frac{c_1^2}{c_2^2} \right)$ for $u_1 = u_D$

weak R-front $\frac{\rho_2}{\rho_1} \approx 1 + \frac{c_2^2}{u_1^2}$ for $u_1 \gg u_R$

strong R-front $\frac{\rho_2}{\rho_1} \approx \frac{u_1^2}{c_2^2} - 1$

weak D-front $\frac{\rho_2}{\rho_1} \approx \frac{c_1^2}{c_2^2} - \frac{u_1^2}{c_1^2}$ for $u_1 \ll u_D$

strong D-front $\frac{\rho_2}{\rho_1} \approx \frac{u_1^2}{c_1^2} \left(1 + \frac{c_2^2}{c_1^4} u_1^2 \right)$



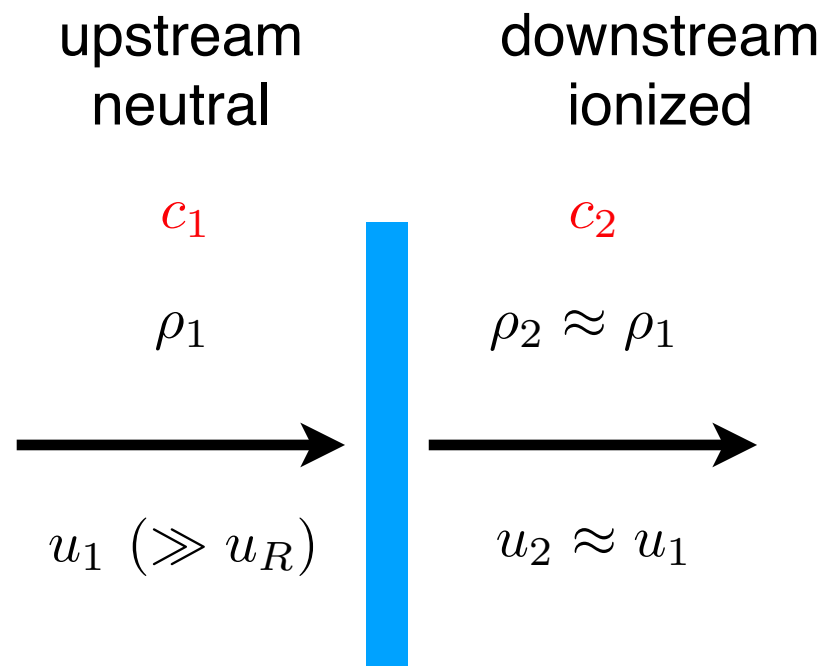
	$u_R \approx 2c_2, \quad u_D \approx \frac{1}{2} \frac{c_1^2}{c_2}$
R-critical	$\frac{\rho_2}{\rho_1} \approx 2$ for $u_1 = u_R$
D-critical	$\frac{\rho_2}{\rho_1} \approx \frac{1}{2} \frac{c_1^2}{c_2^2}$ for $u_1 = u_D$
strong R-front	$\frac{\rho_2}{\rho_1} \approx \frac{u_1^2}{c_2^2}$ for $u_1 \gg u_R$
weak R-front	$\frac{\rho_2}{\rho_1} \approx 1$
weak D-front	$\frac{\rho_2}{\rho_1} \approx \frac{c_1^2}{c_2^2}$ for $u_1 \ll u_D$
strong D-front	$\frac{\rho_2}{\rho_1} \approx \frac{u_1^2}{c_1^2}$

Figure 4.11 [Ryden]

- We note that the four types are not all relevant to H II regions.
 - ▶ For instance, the strong R type means a lower density in the upstream (neutral gas). The strong R-type fronts are in fact unstable (Rayleigh-Taylor instability). In H II regions, the neutral gas has a higher density than the ionized gas. (or the same density at the initial stage).
 - ▶ The strong D type implies that the density in neutral gas increases forever when the ionization front slows down.
- The fronts relevant to the HII regions are R-front and D-front.

Evolution of Ionization Front

[1] Weak R front



We will assume that

$$c_1 = (kT_1/m_H)^{1/2}$$

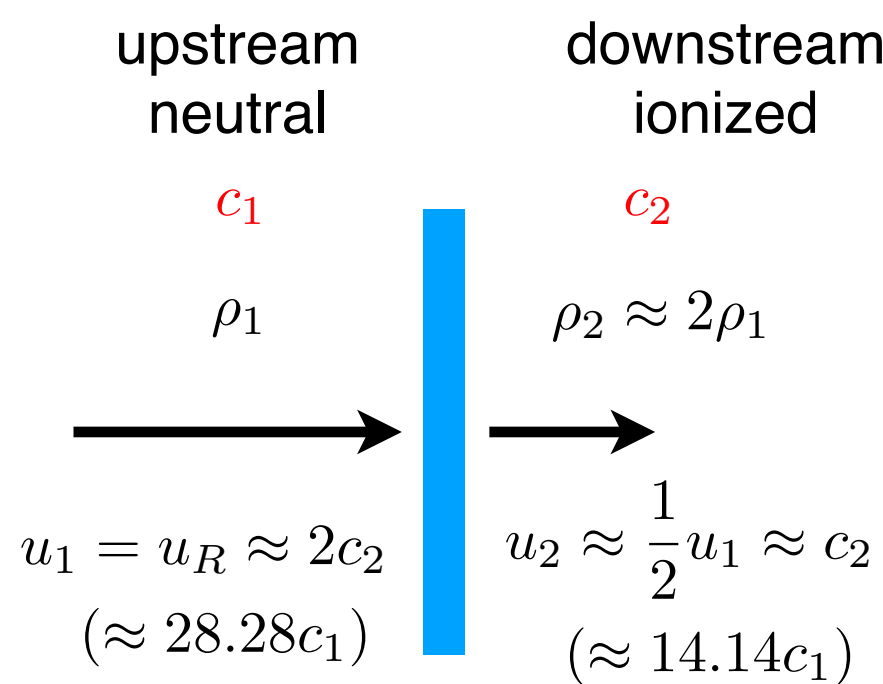
$$c_2 = (2kT_2/m_H)^{1/2} = (2T_2/T_1)^{1/2} c_1 = \sqrt{200} c_1$$

for $T_1 = 10^2 \text{ K}$, $T_2 = 10^4 \text{ K}$

(1) Weak R front:

- Initially, the photon flux J is very large. Thus, u_1 is very large, and the ionization front is initially a weak R-type front. The densities of neutral gas and ionized gas are nearly the same: $\rho_2/\rho_1 \approx 1$. (A weak R-type front compresses the gas only slightly.)
- As the ionization front expands, the flux of ionizing photons steadily decreases, and the propagation speed u_1 of the front slows down.

[2] R-critical front

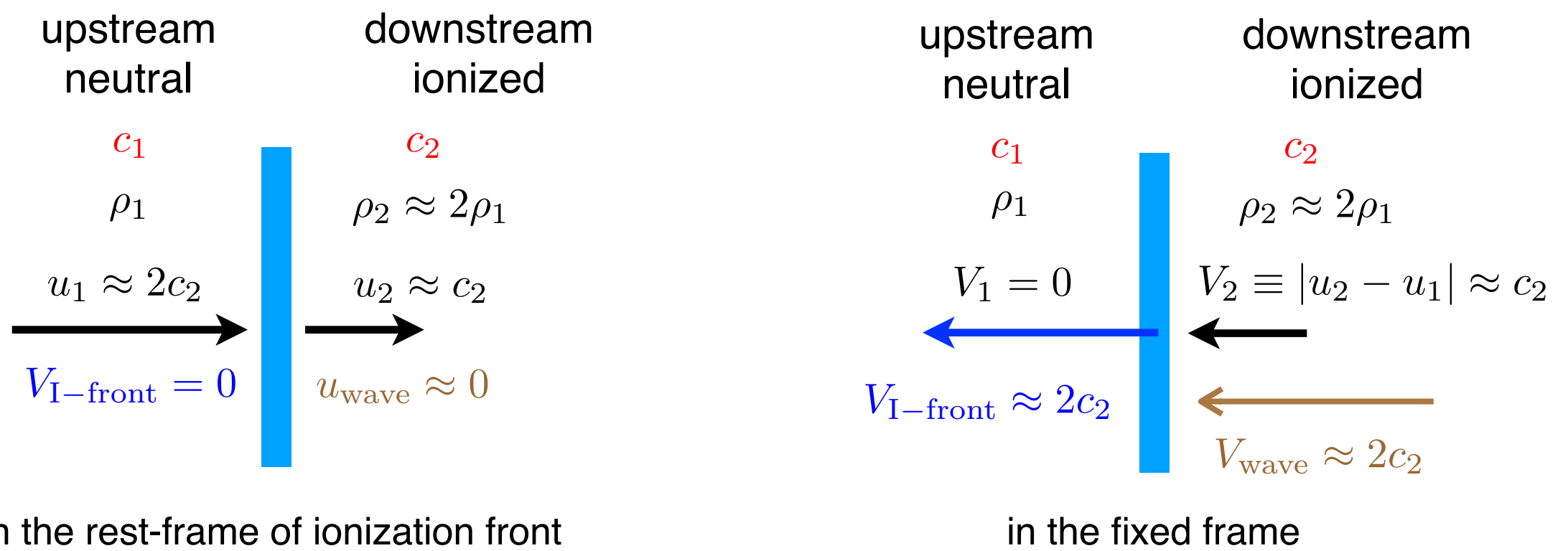


(2) R-critical front:

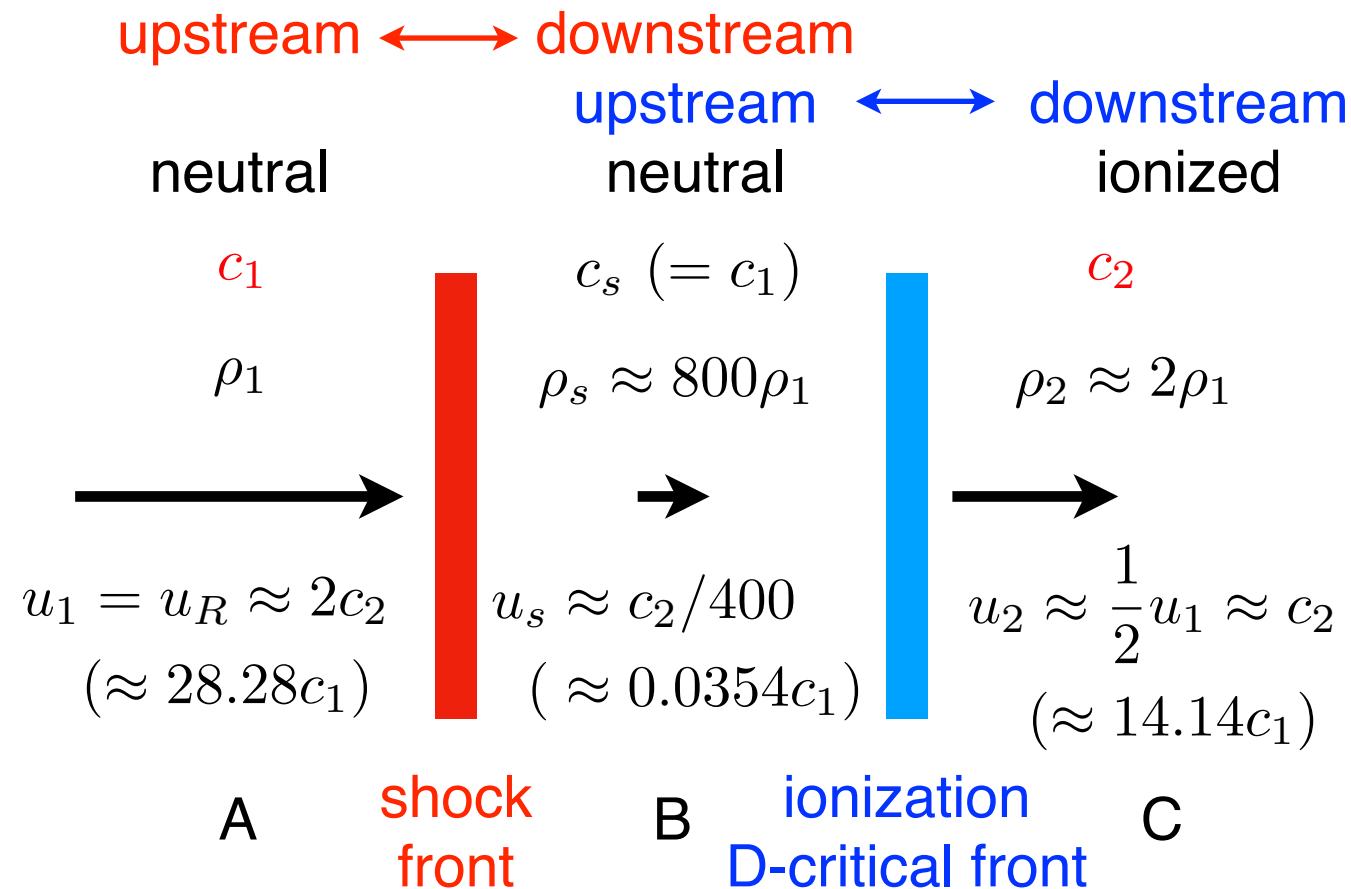
- Eventually, the speed drops to a value $u_1 = u_R \approx 2c_2$.
- At this point, the density ratio has risen to $\rho_2/\rho_1 \approx 2$.
- The speed of the ionized gas is $u_2 \approx (1/2)u_R \approx c_2$ relative to the ionization front, or $u_2 - u_1 \approx -c_2$ in a fixed frame of reference.
- As the ionization front slows down farther, the R-type front can no longer exist.

● How does the evolution proceed once the ionization front becomes R-critical?

- When the R-critical condition is reached, the gas in the H II region just behind the front is moving at a speed equal to $c_2 \gg c_1$.
- This should derive a shock wave into the preionization front gas. Before this point, the large pressure discrepancy between the H II region and the H I region ahead of it has no chance to act dynamically, because the ionization front races ahead with speed u_1 so much faster than a pressure wave can catch it.
- When the ionization front slows down to a speed $u_1 = u_R \approx 2c_2$, however, the pressure wave (moving at a speed c_2 on top of the speed $u_2 \approx c_2$ that the H II fluid itself moves) can catch up with the ionization front and overtake it.
- In doing so, the pressure wave will steepen into a shock wave, thereby compressing the atomic gas behind it into a denser state that the lagging ionization front then has to eat into.



[3] D-critical front



(3) D-critical front:

- As the ionization front slows down farther, the R-type front can no longer exit. What happens next is that ***the R-critical ionization front splits into a pair of fronts (shock front + ionization front)***.
- ***A leading shock front is followed by a D-critical ionization front.*** The shock front is the boundary between two regions of gas with different density, pressure, and temperature, but no necessarily different ionization states. The shock front propagates with a supersonic speed relative to the gas in the upstream of the shock front.

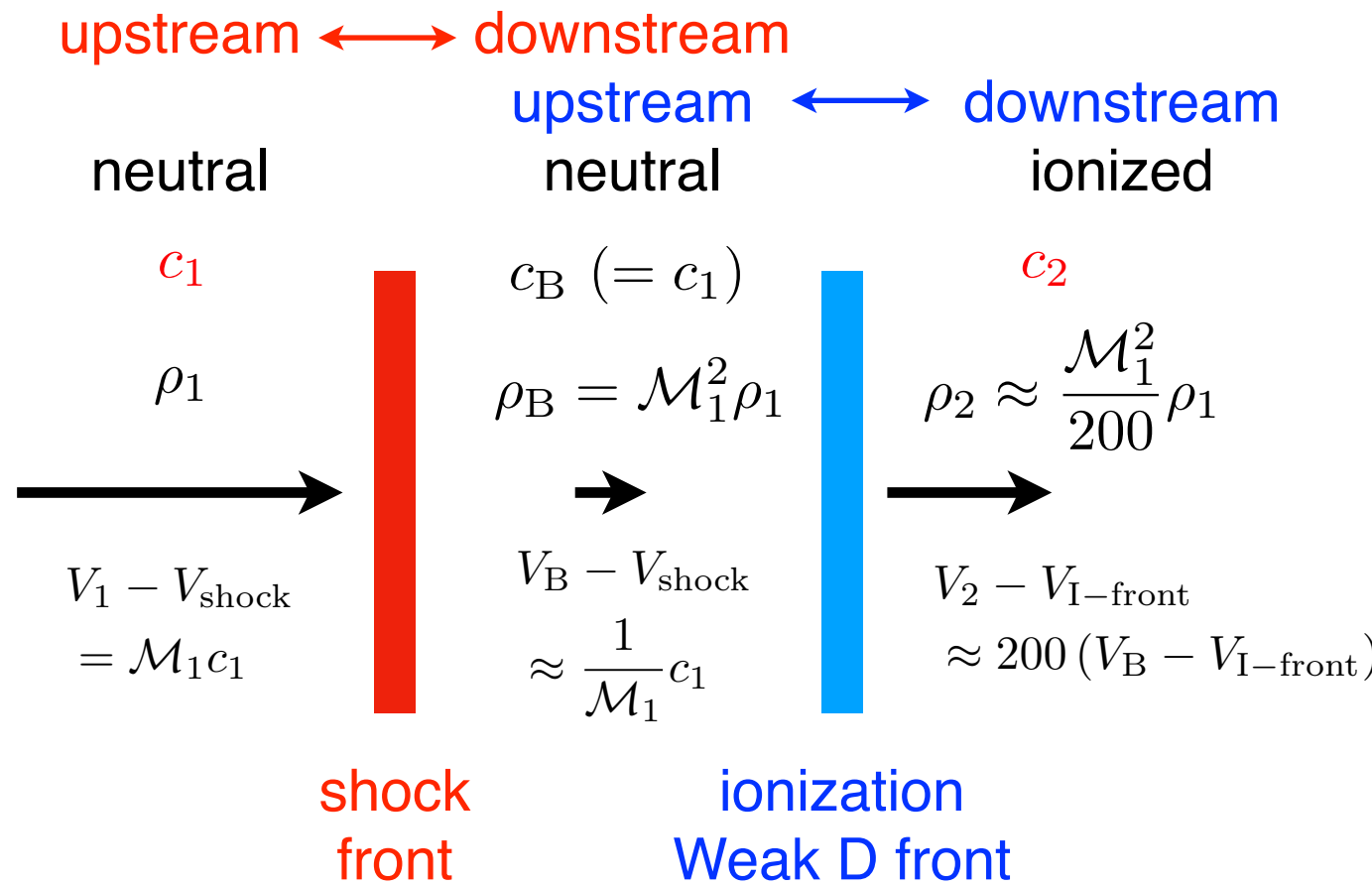
- We will assume ***an isothermal shock***. Then, the sound speed of the shocked region (B) must be $c_s = c_1$ (from the Rankin-Hugoniot jump condition). Then, using the condition for the D-critical, we obtain the density and speed of the shocked region (B):

$$\begin{aligned} \frac{\rho_2}{\rho_s} &\approx \frac{1}{2} \frac{c_1^2}{c_2^2} = \frac{1}{400} & \frac{u_s}{u_2} &= \frac{\rho_2}{\rho_s} \\ \rho_s &\approx 400\rho_2 \approx 800\rho_1 & u_s &\approx \frac{1}{400}u_2 \approx \frac{1}{400}c_2 \approx \frac{1}{\sqrt{800}}c_1 = 0.0354c_1 \end{aligned}$$

$$\longrightarrow \begin{aligned} \rho_s &\approx 800\rho_1 \\ u_s &\approx 0.0354c_1 \end{aligned}$$

- The shocked region (B) has a very high density, and is almost stationary relative to the ionization front. The velocities u_1, u_s, u_2 are measured in the rest-frame of I-front. The R-critical condition between A and C is still satisfied.

[4] Weak D front



(4) Weak D front:

- As the H II region expands still further, the leading shock front gradually weakens and the trailing D-critical front develops into a weak D-type front.
- Notice that the weakest of weak-D ionization fronts corresponds to the density discontinuity:

$$\frac{\rho_2}{\rho_B} = \frac{c_1^2}{c_2^2}$$

This is the condition for the static pressure equilibrium in isothermal gas,

$$\rho_2 c_2^2 = \rho_B c_1^2 \quad (P = \rho c_s^2)$$

the state that we expect for the final Stromgren sphere.

- The condition for the weak D-type front must be satisfied between the regions “B” and “2”.
- In addition to this condition, The shock jump condition should be satisfied between the regions “1” and “B”.
- However, notice that the velocities of shock front and ionization front are different, in general.

$$V_{\text{shock}} \neq V_{\text{I-front}}$$

Intermediate States - expansion phase

- Assumptions:
 - The shocked gas layer is thin.
 - The ionization front follows the shock front and the expansion velocity of ionized sphere is approximately the same as the shock velocity.
- Expansion:
 - The pressure behind a strong “isothermal” shock (high Mach number) is related to the shock velocity:
$$P_s = \rho_0 V_s^2 = n_0 m_H V_s^2$$
 - Now assume that the pressure behind the shock wave is equal to the pressure of the ionized gas (pressure equilibrium).

$$P_i = 2n_i kT = n_i m_H c_i^2 \quad \left(c_i^2 \equiv \frac{2kT}{m_H} \right)$$

$$P_s = P_i \rightarrow V_s^2 = \frac{n_i}{n_0} c_i^2 \rightarrow \frac{V_s^2}{c_i^2} = \frac{n_i}{n_0}$$

-
- We assume that the amount of fresh neutral gas to be ionized is very small. Then, the ionization balance for the region within R gives

$$Q_0 = \frac{4\pi}{3} R^3 n_i^2 \alpha_B \quad \rightarrow \quad R^3 = \frac{3Q_0}{4\pi n_i^2 \alpha_B} = R_s^3 \left(\frac{n_0}{n_i} \right)^2$$

- Combining with $\frac{V_s^2}{c_i^2} = \frac{n_i}{n_0}$, the equation for the expansion of the ionization front is

$$R^3 = R_s^3 \left(\frac{c_i}{V_s} \right)^4$$

$$\rho \equiv R/R_s, \quad \tau \equiv c_i t / R_s \quad \rho^3 \left(\frac{d\rho}{d\tau} \right)^4 = 1 \quad \rightarrow \quad \rho^{3/4} \frac{d\rho}{d\tau} = 1$$

- For a suitable boundary condition, we assume that the initial Stromgren sphere is set up at τ_0 (a very small fraction of the lifetime of the H II region):

$$R = R_s \text{ at } \tau = \tau_0 \quad (\ll 1)$$

- Then, the solution of the differential equation is

$$\rho = \left[1 + \frac{7}{4}(\tau - \tau_0) \right]^{4/7} \quad R = R_s \left(1 + \frac{7}{4} \frac{t - t_0}{R_s/c_i} \right)^{4/7}$$

-
- Expanding velocity is

$$\frac{dR}{dt} = c_i \left(1 + \frac{7}{4} \frac{t - t_0}{R_s/c_i} \right)^{-3/7}$$

- What is the time scale to reach the pressure equilibrium?

$$R(t_{\text{eq}}) = R_f \approx 34R_s$$

$$R_s \left(1 + \frac{7}{4} \frac{t_{\text{eq}}}{R_s/c_i} \right)^{4/7} \approx 34R_s \quad t_{\text{eq}} \approx 273 (R_s/c_i)$$

- The expanding velocity at this point is:

$$V_s = \frac{dR}{dt} = 0.71 c_i \quad \text{at} \quad t_{\text{eq}} = 273R_s/c_i$$

Timescales for typical HII region

- Let's examine the case of an O7V star with

$$Q_0 = 10^{49} \text{ s}^{-1}, \quad n_0 = 10^2 \text{ cm}^{-3}, \quad T = 10^4 \text{ K}$$

- Initial state: recombination time scale $t_{\text{rec}} = (n_0 \alpha_B)^{-1}$

$$R \approx R_s \text{ at } t = t_{\text{rec}}$$

$$R_s \approx 3 \text{ pc} (\approx 10^{19} \text{ cm})$$

$$t_{\text{rec}} \approx 1000 \text{ yr}$$

$$R(t) = R_s \left(1 - e^{-t/t_{\text{rec}}}\right)^{1/3}$$

$$\frac{dR}{dt} = \frac{R_s}{3t_{\text{rec}}} \frac{e^{-t/t_{\text{rec}}}}{(1 - e^{-t/t_{\text{rec}}})^{2/3}}$$

- Expansion phase: expansion timescale $t_{\text{exp}} = R_s/c_i$

expansion velocity : $V_s \leq 0.65 c_i$ at $t \geq t_{\text{exp}}$

$$c_i \approx 10 \text{ km s}^{-1}$$

$$t_{\text{exp}} \approx 3 \times 10^5 \text{ yr} \rightarrow t_{\text{exp}} \approx 200 t_{\text{rec}}$$

$$R = R_s \left(1 + \frac{7}{4} \frac{t - t_0}{R_s/c_i}\right)^{4/7}$$

$$\frac{dR}{dt} = c_i \left(1 + \frac{7}{4} \frac{t - t_0}{R_s/c_i}\right)^{-3/7}$$

- Final state: equilibrium timescale $t_{\text{eq}} \approx 273 R_s/c_i$ (from expansion phase model)

$$R = R_f \text{ at } t = t_{\text{eq}}$$

$$R_f/R_s \approx 34$$

$$t_{\text{eq}} \approx 10^8 \text{ yr} \rightarrow t_{\text{eq}} \approx 300 t_{\text{exp}}$$

Does the Stromgren sphere reach pressure equilibrium?

- Main-sequence lifetime of an ionizing star

$$t_{\text{MS}} \approx 10^{10} \left(\frac{M}{M_{\odot}} \right)^{-2} \text{ yr}$$
$$t_{\text{MS}} \approx 10^7 \text{ yr}$$
$$t_{\text{MS}} \approx 10^7 \text{ yr}$$

- Size

- During the lifetime of an O star, which is less than 10 Myr, interstellar gas moving at 10 km/s will travel less than 100 pc, which is comparable with the diameter of the larger H II regions.
- Thus, before an H II region has expanded very far, its central energy source will be extinguished.

- Time Scale:

- Main-sequence lifetime of an ionizing star is 10 times smaller than the time scale for the pressure equilibrium:

$$t_{\text{MS}} \approx 10^7 \text{ yr} \ll t_{\text{eq}} \approx 10^8 \text{ yr}$$

- It is unlikely that the final state (pressure equilibrium) of H II region can be reached during lifetime of star.

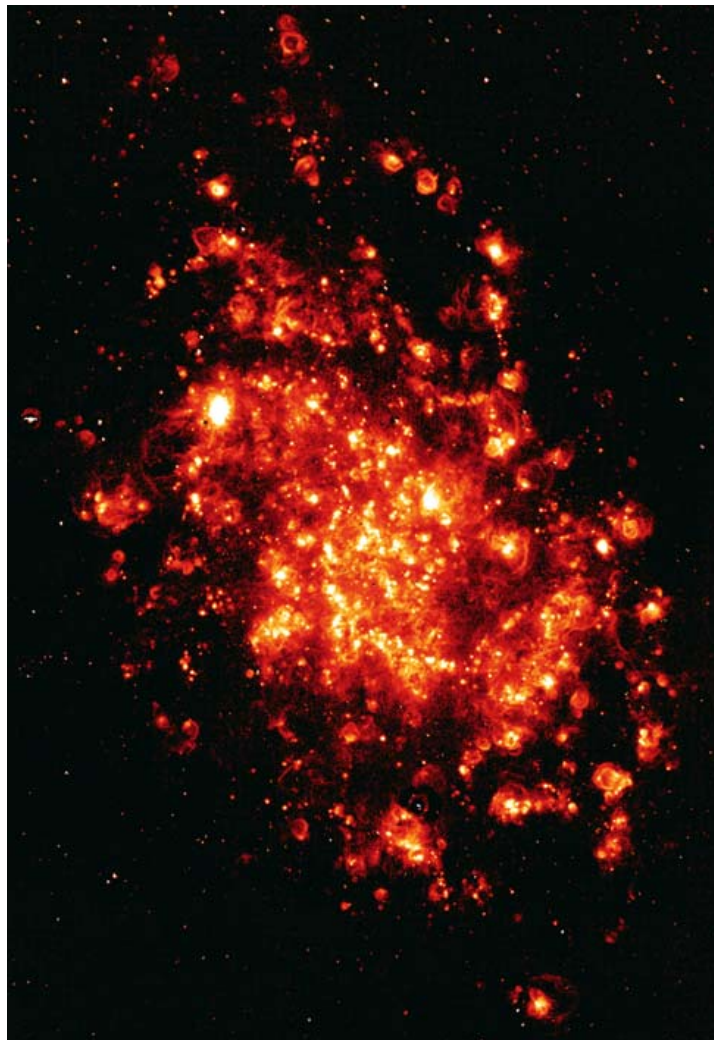
Warm Ionized Medium / Diffuse Ionized Gas

- ***Outside well-defined H II regions, the ISM is known to contain diffuse ionized gas***
 - which can originate either from leaks of ionized gas out of H II regions due to the champagne effect, or from ionization by the UV radiation of isolated hot stars, and perhaps from other mechanisms.
 - In our Galaxy, the DIG is known to contain much more mass than the HII regions. Its total mass is of the order of 1/3 of that of H I.



M51 (NGC5195)
Plate 1 [Lequeux]

B band - blue
V band - green
Ha - red

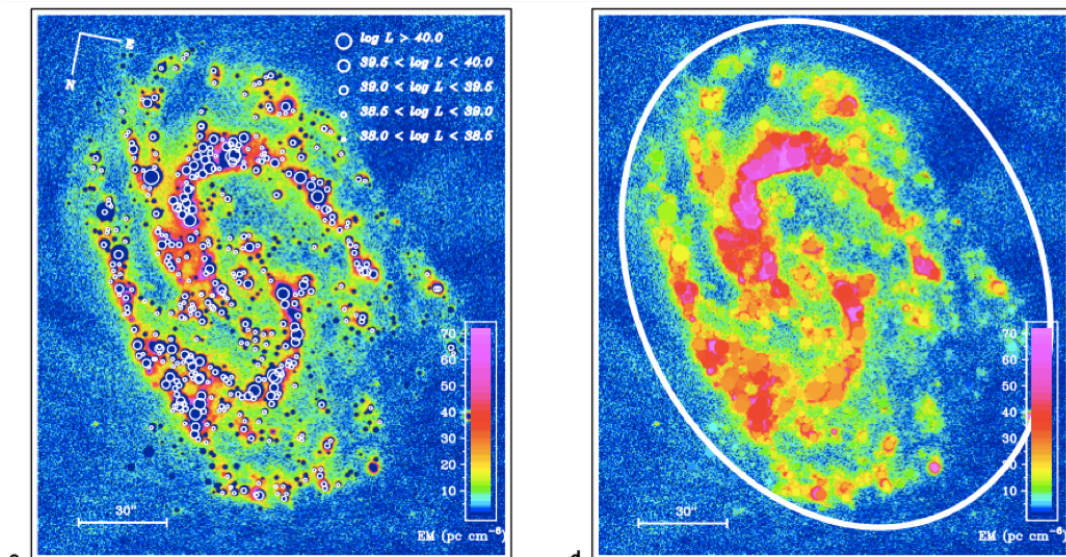


Ionized gas in M33
Plate 10 [Lequeux]

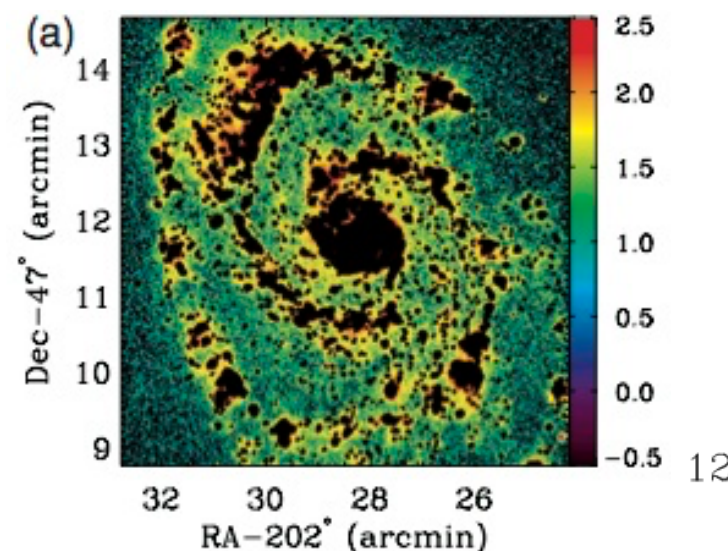
Many bubbles and
the DIG present
almost everywhere
in the central
region.

- ▶ Face-on & edge-on galaxies
- ▶ H α flux of WIM $\sim 20\%-60\%$ of the total H α flux.

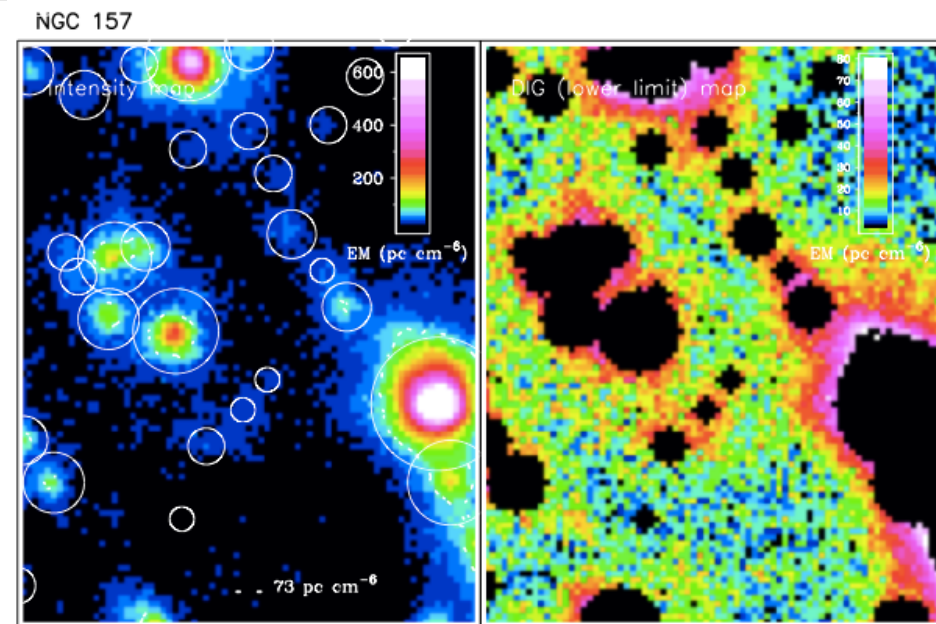
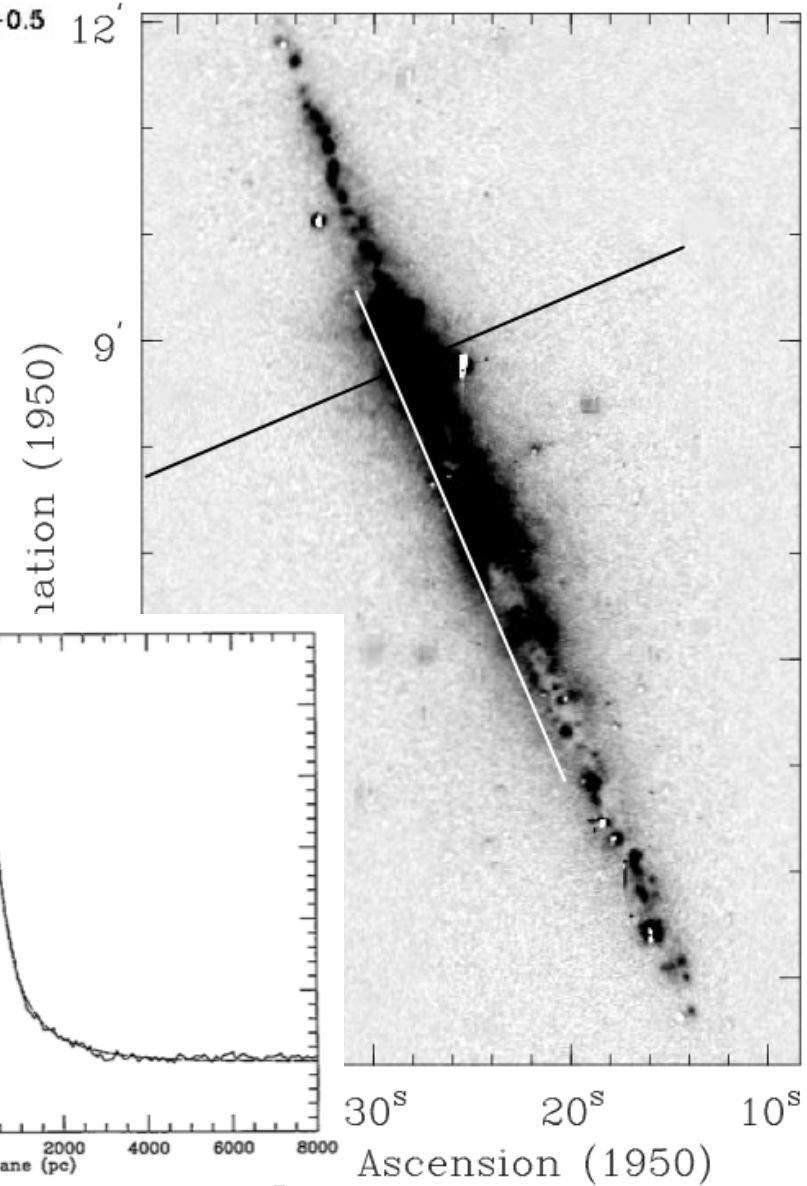
NGC 157 (Zurita e al. 2000)



M 51 (Seon 2009)

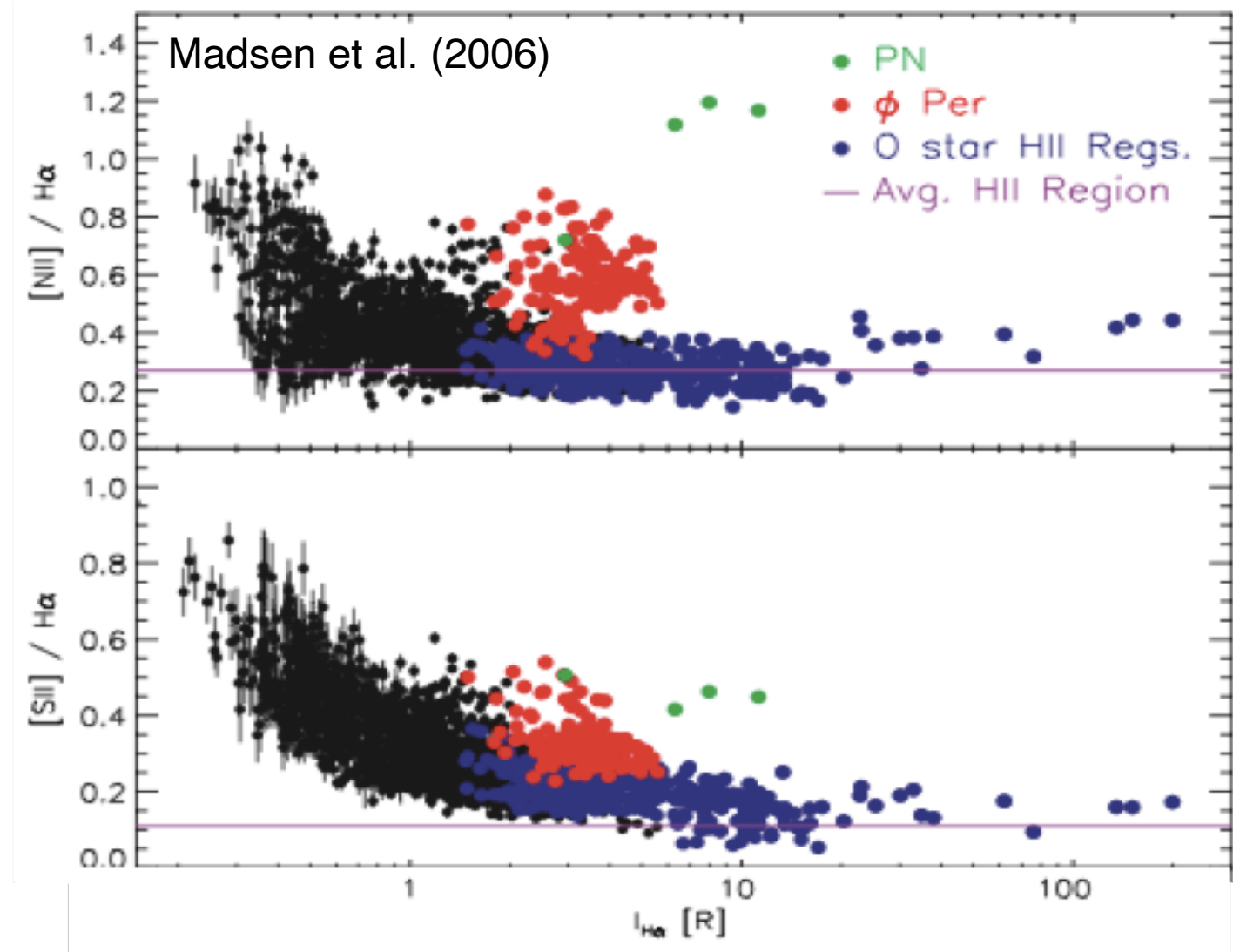
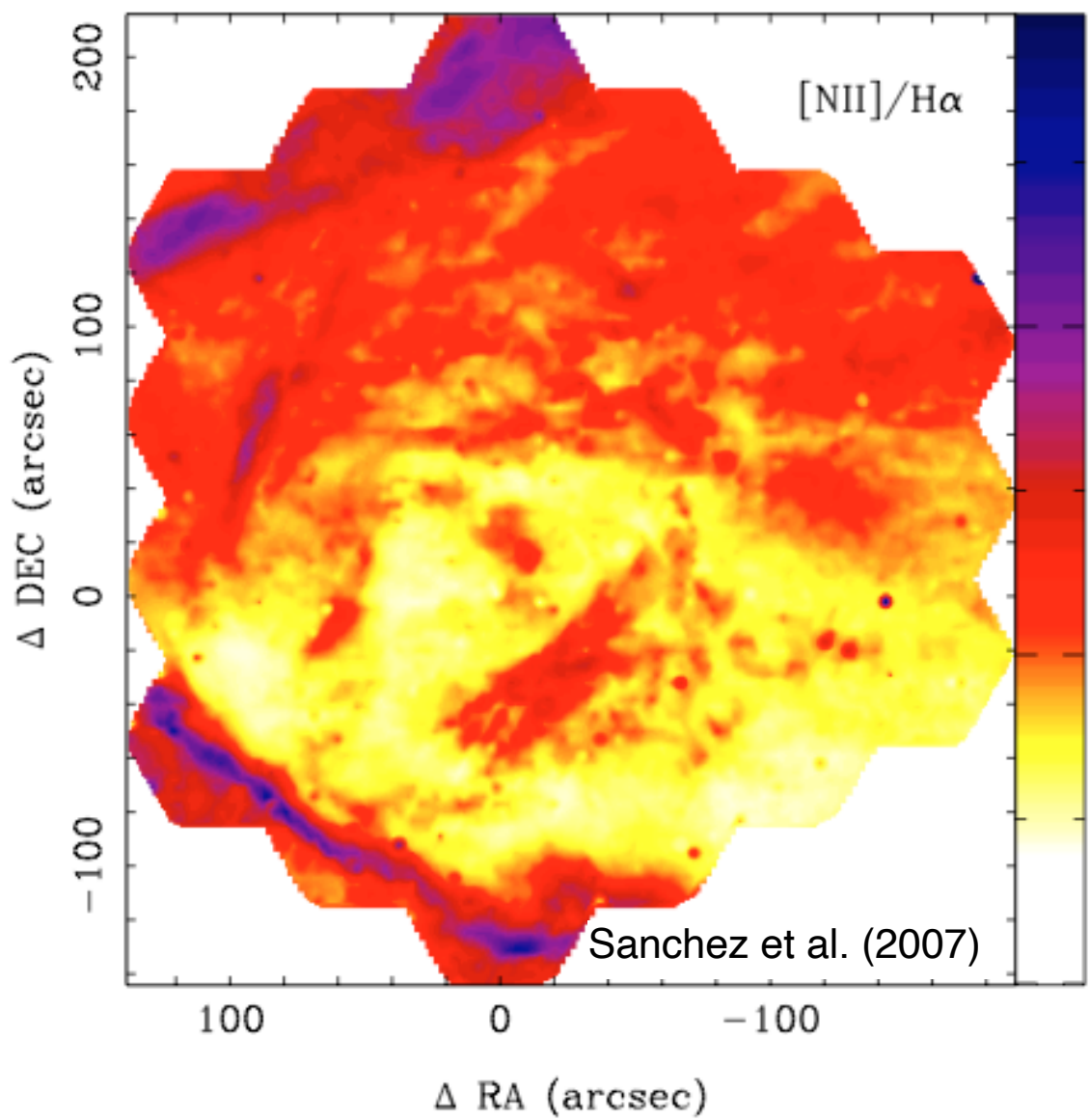


NGC 891 (Rand et al. 1998)

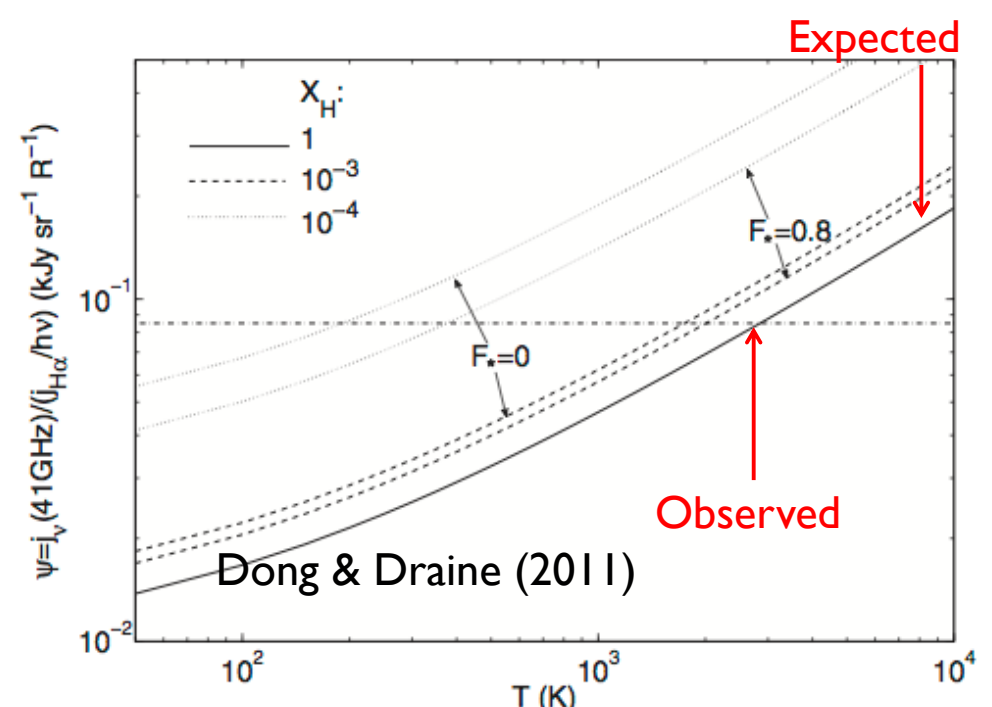
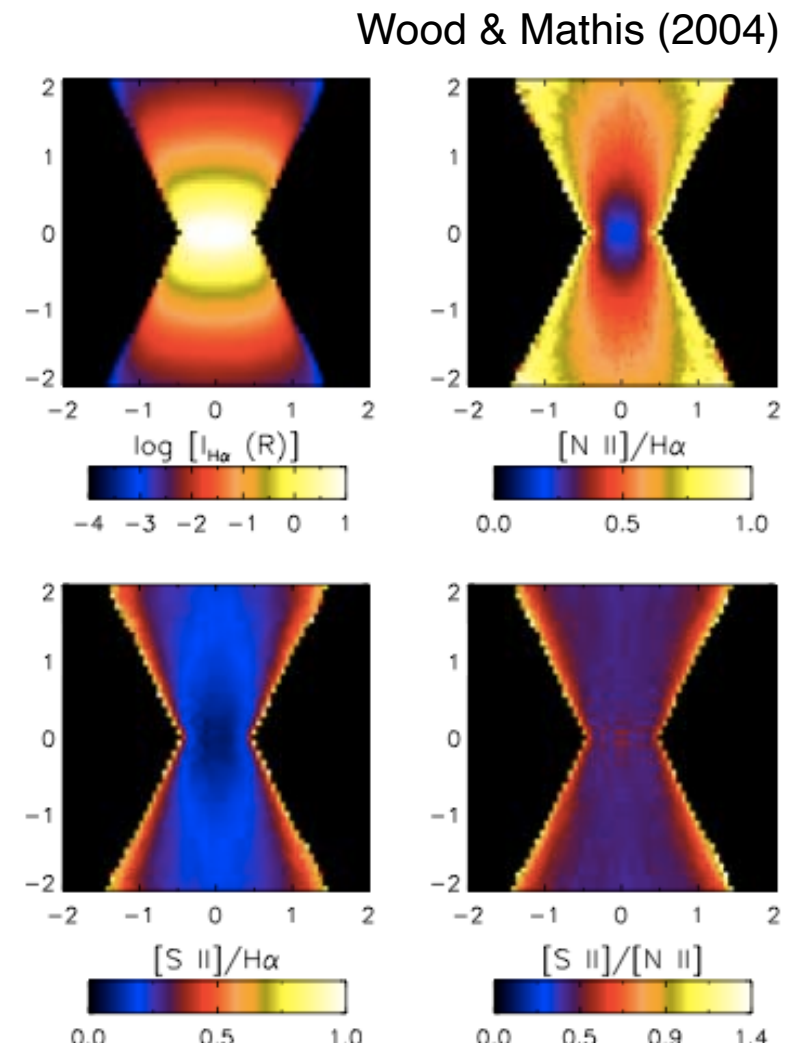


Optical Line Ratios

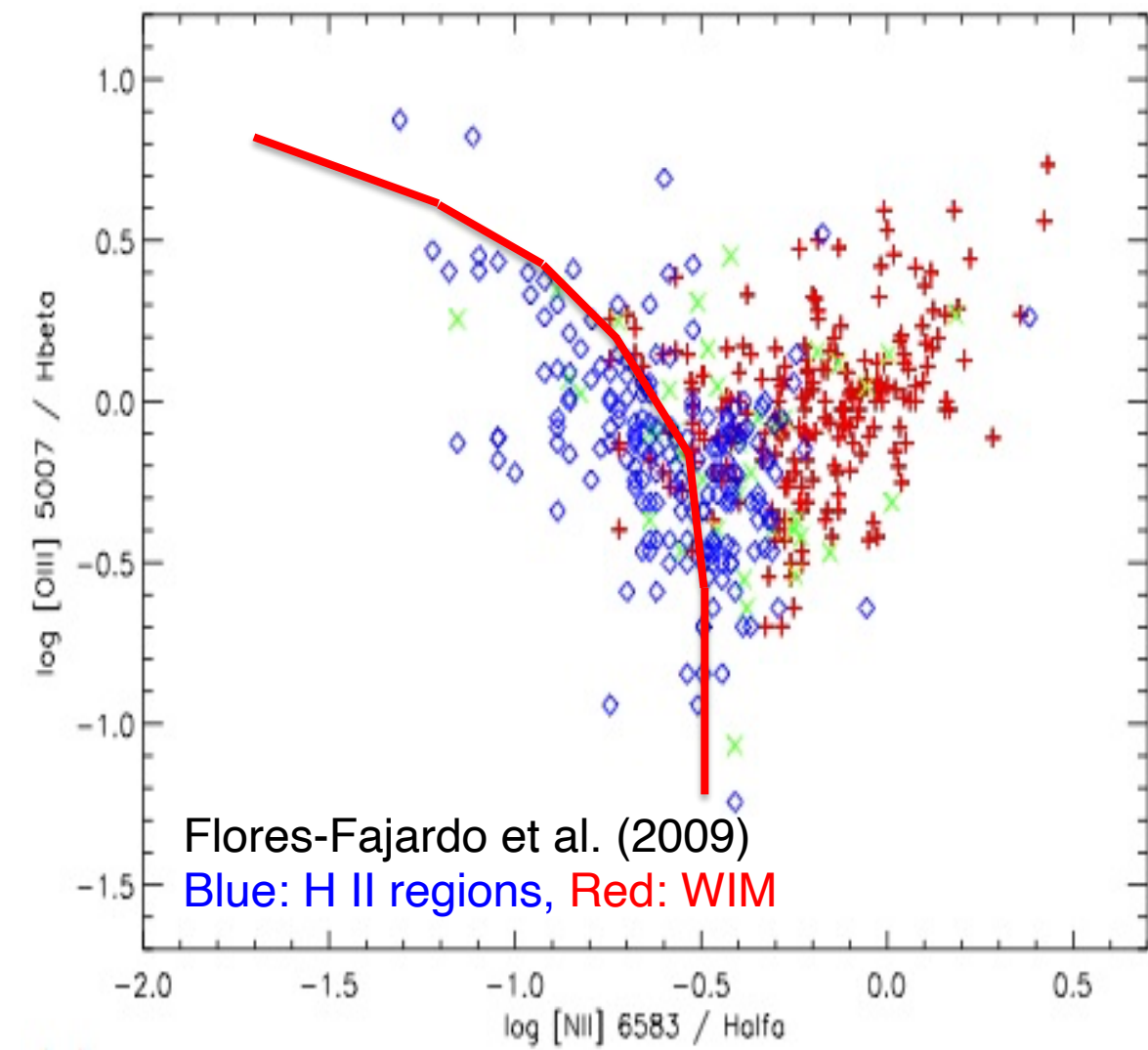
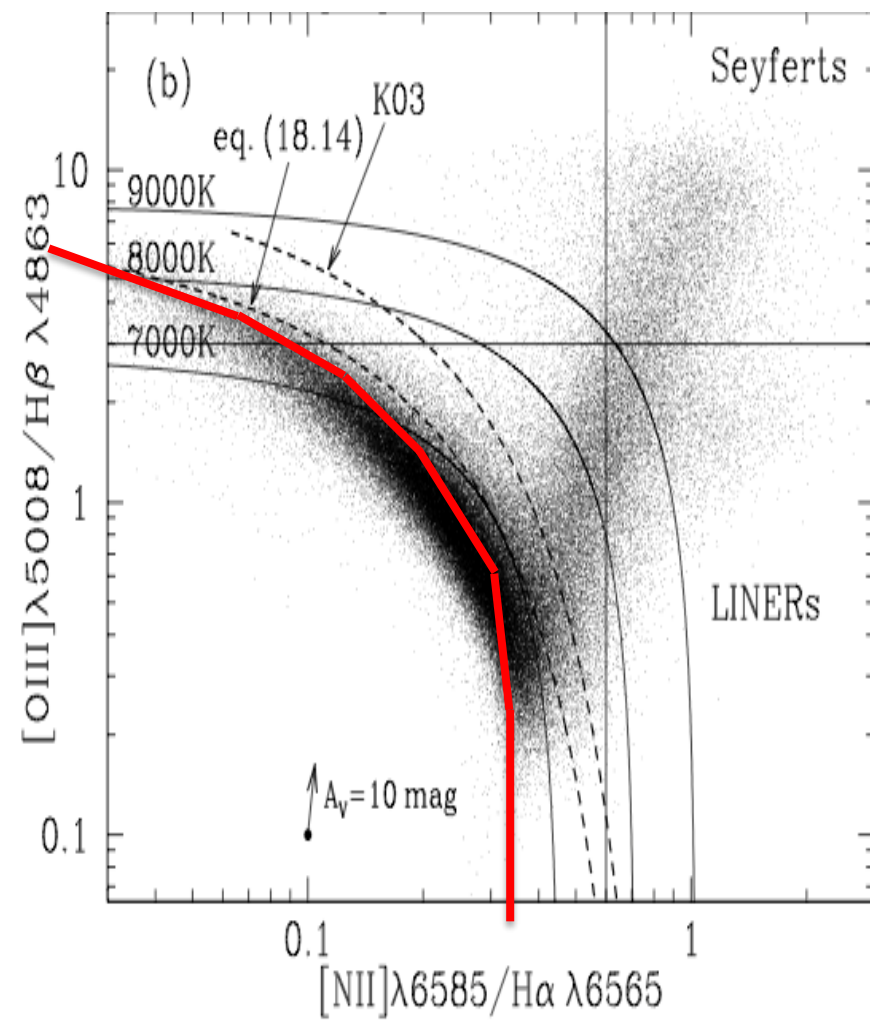
- [N II] $\lambda 6583/\text{H}\alpha$ and [S II] $\lambda 6716/\text{H}\alpha$ in the diffuse regions are generally higher than the ratios in bright H II regions.
 - $[\text{N II}]/\text{H}\alpha \approx 0.25$ and $[\text{S II}]/\text{H}\alpha \approx 0.1$ in bright H II regions
 - $[\text{N II}]/\text{H}\alpha \approx 0.3-0.6$ and $[\text{S II}]/\text{H}\alpha \approx 0.2-0.4$ in the diffuse ISM regions.



- Ionizing Mechanism
 - Only the O stars meet and surpass the power requirements to ionize the diffuse ISM.
 - Density-bounded (leaky) H II regions
 - ▶ Turbulent or clumpy morphology of the ISM
 - ▶ Existence of enormous, H I-free bubbles/holes surrounding the O stars
- However, this mechanism can not explain the free-free radio emission
 - The WMAP data shows that the observed ratio of free-free radio continuum to H α is at least twice smaller than the expected value.
 - Davies et al. (2006, 2009), Dobler & Finkbeiner (2008a,b), Gold et al. (2011)
- See Seon (2009), Seon & Witt (2012), and Dong & Draine (2011) for the possibility of alternative explanations.



Heating source of the WIM



Detailed analyses of the line ratios $[N II]/H\alpha$ and $[S II]/H\alpha$ have been performed to obtain the temperature; it is found to be of the order of 8,000 K.

However, it is also known that WIM is being heated by additional sources. (see the above BPT diagram).

Homework

- The observed spectrum of an HII region has

$$\frac{I(\text{[O III]}4364.4 \text{\AA})}{I(\text{[O III]}5008.2 \text{\AA})} = 0.003 ,$$

$$\frac{I(\text{[O II]}3729.8 \text{\AA})}{I(\text{[O II]}3727.1 \text{\AA})} = 1.2 .$$

- If interstellar reddening is assumed to be negligible, estimate the electron temperature T and the electron density n_e .
- Now suppose that it is learned that there is reddening due to intervening dust with
 $A(4364.4\text{\AA}) - A(5008.2\text{\AA}) = 0.31 \text{ mag}$

Re-estimate T and n_e . You may find it convenient to use the following equations, which will be learned later.

$$\left. \frac{F_{\lambda_2}}{F_{\lambda_1}} \right|_{\text{observed}} = \left. \frac{F_{\lambda_2}}{F_{\lambda_1}} \right|_{\text{intrinsic}} \exp [-(\tau_{\lambda_2} - \tau_{\lambda_1})] \quad \frac{A_{\lambda}}{\text{mag}} = 1.086 \tau_{\lambda}$$